

1962

Molecular Field Relationships to Liquid Viscosity, Compressibility, and Prediction of Thermal Conductivity of Binary Liquid Mixtures.

Harold Vernon Rodriguez

Louisiana State University and Agricultural & Mechanical College

Follow this and additional works at: https://digitalcommons.lsu.edu/gradschool_disstheses

Recommended Citation

Rodriguez, Harold Vernon, "Molecular Field Relationships to Liquid Viscosity, Compressibility, and Prediction of Thermal Conductivity of Binary Liquid Mixtures." (1962). *LSU Historical Dissertations and Theses*. 737.
https://digitalcommons.lsu.edu/gradschool_disstheses/737

This Dissertation is brought to you for free and open access by the Graduate School at LSU Digital Commons. It has been accepted for inclusion in LSU Historical Dissertations and Theses by an authorized administrator of LSU Digital Commons. For more information, please contact gradetd@lsu.edu.

This dissertation has been 62-3663
microfilmed exactly as received

RODRIGUEZ, Harold Vernon, 1932-
MOLECULAR FIELD RELATIONSHIPS TO LIQUID
VISCOSITY, COMPRESSIBILITY, AND PREDICTION
OF THERMAL CONDUCTIVITY OF BINARY LIQUID
MIXTURES.

Louisiana State University, Ph.D., 1962
Engineering, chemical
University Microfilms, Inc., Ann Arbor, Michigan

MOLECULAR FIELD RELATIONSHIPS TO LIQUID VISCOSITY,
COMPRESSIBILITY, AND PREDICTION OF THERMAL
CONDUCTIVITY OF BINARY LIQUID MIXTURES

A Dissertation

Submitted to the Graduate Faculty of the
Louisiana State University and
Agricultural and Mechanical College
in partial fulfillment of the
requirements for the degree of
Doctor of Philosophy

in

The Department of Chemical Engineering

by

Harold Vernon Rodriguez
B.S., Louisiana State University, 1954
M.S., Louisiana State University, 1958
January, 1962

ACKNOWLEDGEMENT

The author wishes to express his gratitude to Dr. Jesse Coates, Head of the Department of Chemical Engineering, for his guidance and assistance in this research.

Special thanks are due to Mr. Larry Morton and the personnel of the Louisiana State University Computer Research Center, for their assistance and time in programming and processing many of the calculations.

The work of Miss Helen Chisholm in the typing of the draft and final copies is gratefully acknowledged.

Finally, the author is deeply indebted to his wife for her encouragement and constant inspiration, and her never-failing tolerance of an often ill-natured spouse.

TABLE OF CONTENTS

	Page
ABSTRACT	ix
CHAPTER	
I INTRODUCTION	1
II THEORETICAL DEVELOPMENT	5
1. The Kardos Equation for Pure Liquids	5
2. Extension of the Kardos Equation to Solutions	8
3. Theory Underlying the Prediction of the Apparent Intermolecular Distance of a Solution	9
4. Prediction of the Apparent Intermolecular Distance	13
5. The Value of the Pure Component Field	16
6. Extension of the Pure Liquid Field Value to Compressibility	17
7. Applications to Viscosity	19
8. Relationship Between Viscosity and Compressibility	22
9. Theory Recapitulated	22
III APPARATUS	24
IV PROCEDURE	36
V RESULTS	38
1. Determination of the Molecular Field Values	38
2. Prediction of the Thermal Conductivity of Binary Liquid Mixtures	51
3. Relationship of the Compressibility to the Field	55
4. Relationship of Viscosity to the Potential Function "m"	55
5. Relationship Between Viscosity and Compressibility	64

VI	DISCUSSION	66
	1. Calculation Error Propagation	66
	2. General Usefulness of the Method for Predicting Thermal Conductivity of Solutions	69
	3. Mode of Interaction	70
	4. Relationship of the Compressibility to the Field Value	71
	5. Relationship of Viscosity to the Potential Function "m"	72
	6. Relationship Between Viscosity, Compressibility, and Molecular Size	73
	7. Additional Comment	74
VII	CONCLUSION	75
	SELECTED BIBLIOGRAPHY	77
	APPENDIX	
A	NOMENCLATURE	81
B	SAMPLE CALCULATIONS	84
C	NOTES ON FIELD THEORY	88
D	TABULATED RESULTS	91
E	INDEX TO LITERATURE DATA	107
	VITA	108

LIST OF TABLES

Table		Page
I	Molecular Field Values at 25°C and 1 Atmosphere	52
II	Thermal Conductivity Values for the Acetone-Ethanol System at 25°C and 1 Atmosphere	53
III	Thermal Conductivity Values for the Acetone-Chloroform System at 25°C and 1 Atmosphere	54
IV	Thermal Conductivity Values for the Methanol-Water System at 25°C and 1 Atmosphere	56
V	Thermal Conductivity Values for the Ethanol-Water System at 25°C and 1 Atmosphere	57
VI	Thermal Conductivity Values for the Propanol(n)-Water System at 25°C and 1 Atmosphere	58
VII	Thermal Conductivity Values for the Glycerine-Water System at 25°C and 1 Atmosphere	59
VIII	Thermal Conductivity Values for the Acetone-Water System at 25°C and 1 Atmosphere	60
IX	Thermal Conductivity Values for the Ethyl Ether-Chloroform System at 25°C and 1 Atmosphere	61
X	Results for the Methanol-Water System at 25°C and 1 Atmosphere	91
XI	Results for the Ethanol-Water System at 25°C and 1 Atmosphere	92
XII	Results for the Propanol(n)-Water System at 25°C and 1 Atmosphere	93
XIII	Results for the Acetone-Water System at 25°C and 1 Atmosphere	94
XIV	Results for the Glycerine-Water System at 25°C and 1 Atmosphere	95

Table		Page
XV	Results for the Ethyl Ether-Chloroform System at 25°C and 1 Atmosphere	96
XVI	Results for the Acetone-Benzene System at 25°C and 1 Atmosphere	97
XVII	Results for the Acetic Acid-Water System at 25°C and 1 Atmosphere	98
XVIII	Results for the Benzene-Carbon Tetrachloride System at 25°C and 1 Atmosphere	99
XIX	Results for the Ethylene Glycol-Water System at 25°C and 1 Atmosphere	100
XX	Results for the Ethyl Ether-Benzene System at 25°C and 1 Atmosphere	101
XXI	Results for the Acetone-Chloroform System at 25°C and 1 Atmosphere	102
XXII	Results for the Acetone-Ethanol System at 25°C and 1 Atmosphere	103
XXIII	Data for Figure 28	104
XXIV	Data for Figure 29	105
XXV	Data for Figure 30	106

LIST OF FIGURES

Figure		Page
1	Initial Arrangement of Molecules in a Liquid	5
2	Arrangement of Molecules in a Liquid for the Transfer of Thermal Energy	6
3	Arrangement of Molecules in a Liquid for the Further Transfer of Thermal Energy	6
4	Lattice Structures for Two Components of a Possible Solution	10
5	Lattice Structure for the Solution of the Two Components	11
6	Variation of the Force Field Between Two Molecules with Distance	19
7	Illustration of the Graphical Difference of the Plot of Average Field Value Versus Composition	21
8	Thermoconductimetric Apparatus for Liquids	25
9	General View of the Apparatus	26
10	Apparatus in Operation	27
11	Apparatus Disassembled	28
12	Top View of the Hot Bar	29
13	Water Baths	30
14	Potentiometer and Galvanometer	31
15	Refractometer	32
16	Intermolecular Distance Versus Composition for Aqueous Solutions	39
17	Intermolecular Distance for Aqueous Solutions	40
18	Intermolecular Distance Versus Composition for Organic Solutions	41

Figure		Page
19	Excess Intermolecular Distance Versus Composition for Aqueous Solutions	42
20	Excess Intermolecular Distance Versus Composition	43
21	Excess Intermolecular Distance Versus Composition	44
22	Excess Free Energy Versus Composition for Aqueous Solutions	45
23	Excess Free Energy Versus Composition for the Glycerine-Water System	46
24	Excess Free Energy Versus Composition	47
25	Molecular Field Value Versus Composition for Aqueous Solutions	48
26	Molecular Field Value Versus Composition for Aqueous Solutions	49
27	Molecular Field Value Versus Composition for the Chloroform-Ethyl Ether System	50
28	Generalized Correlation Between Field, Compressibility, and Molecular Size	62
29	Generalized Correlation Between dF/dL_{CC} , Viscosity, and Molecular Size	63
30	Correlation Between Compressibility, Viscosity, and Molecular Size for Three Series of Compounds	65

ABSTRACT

This work originated in an attempt to predict the thermal conductivity of binary liquid mixtures by use of the Kardos equation, an equation which proved successful for pure liquids. The Kardos equation contains a term for the intermolecular distance, the distance between the surfaces of the molecules, and hence its application to solutions was prevented by the lack of an estimate of the effective intermolecular distance in a solution. The main effort then, was directed toward developing a method for estimating that distance.

It was theorized that in the mixing of two liquids to form a non-ideal solution, the molecules move closer together or farther apart than would be the case for an ideal solution. The actual effective intermolecular distance, as determined from measurement of the physical properties in the Kardos equation, when subtracted from an ideal intermolecular distance, defined as the mole fraction weighted intermolecular distance, yields what was termed the excess intermolecular distance. The excess intermolecular distance is that distance moved by the molecules in departing from ideal behavior.

The excess Gibbs free energy for a non-ideal solution is the maximum work, exclusive of pressure-volume work, involved in the

exhibition of the non-ideal behavior. It was further theorized that this work is the result of the molecules moving through their force fields over the excess intermolecular distance. Consequently it became possible to define the average molecular field value, over the excess intermolecular distance, as the excess free energy divided by the excess intermolecular distance. This average field is a function of composition; extrapolation to the pure component compositions yields the field values for those pure components.

Once the field value has been determined for a liquid, the value of the average field, when that liquid is mixed with another miscible liquid whose field value is known, can be determined from the probability of occurrence of the possible interactions between molecules. The calculation process can now be reversed to calculate the excess intermolecular distance, and then the intermolecular distance for use in the Kardos equation. This method predicted the thermal conductivity of eight binary mixtures to within an average error of $\pm 3.6\%$, with a maximum error of 12%.

The use of the molecular fields was extended to the compressibility of pure liquids, and a successful correlation was found as predicted by a theoretical derivation. The extension of the theory to include compressibility provided a means of predicting the molecular field value. This means of predicting the molecular field value results in an error in predicted thermal conductivity of the order of 8%.

A method utilizing graphical differentiation of the curves of excess free energy and excess intermolecular distance versus composition permitted a further extension of the theory to include viscosity of liquids. A relationship was found between the rate of change of the molecular field with distance and the viscosity of the liquid over a three thousand fold change in viscosity.

Finally, a correlation was found between viscosity and compressibility within a family of compounds. This correlation was predicted through the common parameter of the molecular field variation.

CHAPTER I

INTRODUCTION

This study originated in an attempt to predict the thermal conductivities of binary solutions as functions of their compositions, from a knowledge of the thermal conductivities of the pure components and the variation with composition of certain solution properties. It evolved into a study of intermolecular distances and force fields, and their relationships to thermal conductivity, viscosity and compressibility.

The evolution of this work proceeds from studies of the thermal conductivity of pure liquids. The most successful method for predicting the thermal conductivity of a pure liquid to date is the Kardos equation with the Sakiadis-Coates modification:²¹

$$k = C_p U_s \rho L \quad (1)$$

where

- | | | |
|----------------|---|---|
| k | - | thermal conductivity, Btu/hr-ft ² -°F/ft |
| C _p | - | heat capacity, Btu/lb _m -°F |
| U _s | - | velocity of sound in the liquid, ft/hr |
| ρ | - | density, lbs _m /ft ³ |
| L | - | distance between the surfaces of the molecules, ft. |

The Sakiadis-Coates modification of the Kardos equation consists of the use of X-ray diffraction studies to determine the size of the molecule itself. From this and density measurements, and by assuming a certain orientation of the molecules in the liquid, the distance between the molecular surfaces, L , can be determined.

The thermal conductivities of 42 liquids were predicted by equation (1) with an average deviation of $\pm 2.6\%$ and a maximum deviation of $\pm 6\%$.

With the success of this method for predicting the thermal conductivities of pure liquids, the next logical step was the development of a method for predicting the thermal conductivities of solutions.

Two fairly successful empirical methods have been presented for binary solutions. One is the equation of Fillippov and Novoselova:³

$$k_s = k_2 w_2 + k_1 w_1 - 0.72 (k_2 - k_1) w_2 w_1 \quad (2)$$

where

k - thermal conductivity

w - weight fraction

subscripts

$s, 1, \text{ and } 2$ - solution, component 1 and component 2.
Component 2 is the component having the higher thermal conductivity.

Equation (2) was developed with data on four organic binary solutions: benzene-ethyl ether, benzene-methyl chloride, benzene-carbon tetrachloride, and chloroform-carbon tetrachloride. A later report⁴

specified that the value of the constant in equation (2) should be 0.72 for non-associated solutions, and 0.76 for associated solutions.

The other successful empirical equation is that of Jordan and Coates:¹⁰

$$\ln k_s = w_1 \ln k_1 + w_2 \ln k_2 + w_1 w_2 \ln D \quad (3)$$

where

$$D = e^{(k_2 - k_1) - \frac{(k_2 + k_1)}{2}}$$

Equation (3) must be used with engineering units of Btus, hrs, feet, and degrees Fahrenheit.

Equation (3) predicted the values of thermal conductivity for twelve binary organic mixtures to within $\pm 2\%$, and for nine binary water-organic solutions to within $\pm 3\%$.

However practical these two methods may be, both have one obvious defect. They are equations of curves which will have a symmetrical deviation from a linear relationship between the thermal conductivity and composition, and hence cannot possibly predict the correct values for a system which deviates in any other manner. Although such systems are rare, they nonetheless do exist, e.g.: acetone-carbon-disulfide. The rarity of this type deviation accounts in part for the general success of equations (2) and (3). Riedel acknowledged this difficulty and did not attempt to determine a generalized correlation for his work.¹⁵

A second factor which contributes to the success of any

empirical relation for solution thermal conductivity is that in many instances, particularly with organic systems, the deviation from a linear relationship is often very small, of the order of only three to five per cent. Any reasonable correction factor to a basically linear function will yield seemingly good results.

A method is presented in this work for predicting the thermal conductivity of a solution, regardless of the type of variation with composition or of the type solution. It is an extension of the Kardos equation to solutions, and is founded on a theoretical basis. Unfortunately, because of the many factors involved in the Kardos equation, the method is not as practical, nor as accurate as the equation of Jordan and Coates, and for general purposes, equation (3) is the recommended relation.

A brief presentation of theoretical background information on force fields is to be found in Appendix C.

CHAPTER II

THEORETICAL DEVELOPMENT

1) The Kardos Equation for Pure Liquids

The foundation for the development which follows is the Kardos equation, which predicts the thermal conductivity of pure liquids. The Kardos equation is developed with the aid of a simplified model of the liquid state. This model is presented as an aid to visualization, and is not intended to be an exact representation of the situation or configuration in the liquid state.

Consider the following initial arrangement of molecules of a pure liquid, in which there exists a temperature gradient:

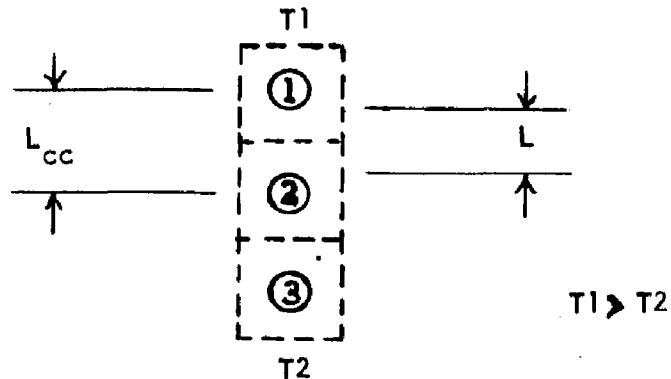


Figure 1

The dotted lines of Figure 1 indicate areas of confinement. "L" is the average distance between the surfaces of the molecules; " L_{cc} " is the center-to-center distance between the molecules. These molecules are in a state of constant agitation, and the next position

might well be:



Figure 2

Molecule 1 has moved upward to contact a hotter molecule above it, molecule 2 has moved downward and collided with upcoming molecule 3. There is a transfer of energy to 1, and from 2 to 3.

Now 1 and 3 begin their rebound downward paths and 2 begins to travel upward.

The next collision position is:

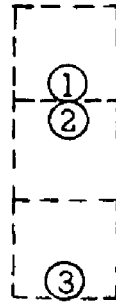


Figure 3

Here molecule 1 transfers its excess energy to 2, and 3 transfers energy to the cooler molecule below it.

This mechanism of energy transfer continues as long as the thermal gradient exists. There is little lateral motion since the thermal gradient is in the vertical direction.

Down the column of molecules pictured above, there is an energy drop per molecule across the distance L of:

$$U = - \left[\frac{d(Q/N)}{dL_{cc}} \right] L \quad (4)$$

where

Q = heat content per mole

N = Avagadros number

or

$$U = -L \left[\frac{d(Q/N)}{dT} \right] \left[\frac{dT}{dL_{cc}} \right] \quad (5)$$

Assuming the energy is transmitted through the liquid with the velocity of sound, the rate of energy transfer in the column of molecules is:

$$q = -L \left[\frac{d(Q/N)}{dT} \right] \left[\frac{dT}{dL_{cc}} \right] \left[\frac{U_s}{L_{cc}} \right] \quad (6)$$

where U_s = velocity of sound

The rate per unit area is

$$\frac{q}{A} = -L \left[\frac{d(Q/N)}{dT} \right] \left[\frac{dT}{dL_{cc}} \right] \left[\frac{U_s}{L_{cc}} \right] \left[\frac{1}{(L_{cc})^2} \right] \quad (7)$$

The well-known Fourier law is:

$$\frac{q}{A} = -k \frac{dT}{dS} \quad (8)$$

where S = distance

Substituting equation (7) into equation (8) and solving for thermal conductivity yields:

$$k = L \left[\frac{d(Q/N)}{dT} \right] \left[\frac{U_s}{(L_{cc})^3} \right] \quad (9)$$

Also:

$$\left[\frac{d(Q/N)}{dT} \right]_P = \left[\frac{MC_p}{N} \right] \quad (10)$$

where

M = molecular weight

C_p = heat capacity, unit mass basis

and:

$$(L_{cc})^3 = \frac{M}{\rho N} \quad (11)$$

where ρ = density, mass per unit volume

Substitution of equations (10) and (11) into (9) yields:

$$k = C_p U_s \rho L \quad (12)$$

Equation (12) is the Kardos equation for predicting the thermal conductivity of pure liquids.

A method for estimating L is presented in the literature²¹.

The method assumes certain molecular shapes and configurations in the liquid.

The thermal conductivities of 42 pure liquids were predicted with the Kardos equation with an average deviation of $\pm 2.6\%$ and a maximum deviation of $\pm 6\%$.

2) Extension of the Kardos Equation to Solutions

Since the Kardos equation proved successful for pure liquids, its application to solutions became an interesting possibility.

To apply the Kardos equation to a solution, the solution is considered as being composed of "average" molecules. At a given composition, the average molecule is defined as one which would have the same specific heat as the solution, which would propagate sonic energy with the same velocity as the solution, which would have the same density as the solution, and finally, one whose intermolecular distance would be the same as the apparent intermolecular distance in the solution. The apparent intermolecular distance in the solution is that value of intermolecular distance which is consistent with the thermal conductivity of the solution, the Kardos equation and the solution properties. This reasoning would be circular were it not for the fact that the apparent intermolecular distance may be determined by an independent method presented in the following section.

3) Theory Underlying the Prediction of the Apparent Intermolecular Distance of a Solution

Three of the four physical properties of a solution necessary for using the Kardos equation could be measured experimentally, but the fourth, the intermolecular distance, could not be. It became necessary to develop a method for predicting it; indeed, this became the primary objective of the investigation.

Consider two pure liquids, the separate components of a possible solution. In keeping with the simplified model used in the development of the Kardos equation, the liquid molecules are considered

as being in a regular lattice structure:



Figure 4

Now the components are mixed, but in a particular manner. They are mixed as if there were no distorting force field interactions between unlike molecules. That is, the only factors affecting the resulting spacing on the mixture lattice are the spacings of the original components, L_1 and L_2 , and the composition of the mixture. The resulting spacing is the same as if the solution were ideal and hence is termed L_i .

If

$$L_1 = L_2 \quad (13)$$

then

$$L_i = L_1 = L_2 \quad (14)$$

In general L_i is defined by:

$$L_i = x_1 L_1 + x_2 L_2 \quad (15)$$

where x = mole fraction

The mixture lattice is considered regular and undistorted. It may be considered as the lattice structure necessary for the average molecules previously defined. The configuration is:

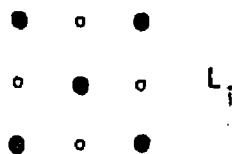


Figure 5

Now the lattice is held rigid and the distorting interactions are added. This places the system under tension (assuming a net attractive force). Now the lattice is released from its rigidity and allowed to contract to an equilibrium position. Energy will be released as a result of the motion of the molecules in the force fields, and there will be a new, smaller lattice spacing. The lattice is still considered regular and undistorted. This new spacing between the molecules is assumed to be the same as the apparent intermolecular distance of the Kardos equation, and, according to previous nomenclature, is designated "L".

In going from the pure components to the final mixture reversibly at constant temperature and pressure, the maximum amount of work, other than expansion work, is given by the Gibbs free energy change:

$$\Delta G = \Delta H - T\Delta S = -W_m + P\Delta V \quad (16)$$

The change in free energy in going from the pure components to the tensed lattice is the same as that for an ideal solution:

$$\Delta G_i = -T\Delta S_i = -W_{mi} \quad (17)$$

The change in free energy in going from the tensed lattice to the final mixture is the difference between equations (16) and (17), and is the excess free energy:

$$G^E = (\Delta G - \Delta G_i) = \Delta H - T(\Delta S - \Delta S_i) \quad (18)$$

$$G^E = -W_m + W_{mi} + P\Delta V \quad (19)$$

The excess free energy then gives the maximum work of moving the molecules in their force fields over the distance $(L_i - L)$.

Maximum work in a force field is given by:

$$dW_m = \vec{F} \cdot d\vec{S} \quad (20)$$

where

\vec{F} = field, a vector quantity and a function of distance

\vec{S} = distance in a given direction, a vector quantity

Thus, if G^E is on a mole basis:

$$G^E = N \int \vec{F} \cdot d\vec{S} \quad (21)$$

Since the molecular field is a function of distance, it is necessary to know this function in order to be able to integrate equation (21).

Several functions for molecular force fields have been proposed, none of which is entirely satisfactory. For the purpose of this discussion an average force field will be assumed over the distance $(L_i - L)$, its value given by:

$$F_m = \frac{G^E}{N L^E} \quad (22)$$

where

F_m = average molecular force field over the distance,
 L^E

L^E = $(L_i - L)$; note that this is not the customary
 definition of an excess function.

Equation (22) assumes the motion always parallel to the field. Excess free energy may be calculated in the usual manner from activity coefficients:

$$G^E = RT (x_1 \ln \gamma_1 + x_2 \ln \gamma_2) \quad (23)$$

where

R = gas content
 T = temperature
 x = mole fraction
 γ = activity coefficient

Subscripts 1 and 2 refer to components 1 and 2, respectively.

The value of the molecular field as given by equation (22) is a crude approximation only. However, later work shows that it is sufficient for the prediction of thermal conductivities. Further discussion of the fields of the pure components, which may be obtained exactly, and their applications to compressibility and viscosity follow in sections 5, 6, and 7.

4) Prediction of the Apparent Intermolecular Distance

As discussed in Appendix C, it is necessary to define a force field with respect to some reference. In the case of a pure liquid, the

field of one molecule would be with respect to a similar molecule. In a solution, however, it becomes necessary to consider the various possible interactions between molecules. For instance, if in a mixture of A and B, a molecule of A approaches a molecule of B, the effect of A's field on B is quite likely to be very much different than it would be on another molecule of A. Hence the molecular field of A, defined in terms of another molecule of A, cannot be readily applied to determine A's effect on B. F_m , defined by equation (22) is the net result of all possible types of interactions.

Consider the possible two-body interactions in a binary solution of A and B. There are the A-A interactions, the B-B, the A-B and the B-A. The probability of an A-A interaction is $X_A X_A$. Similarly, the probability of the B-B interaction is $X_B X_B$, the A-B interaction is $X_A X_B$, and the B-A interaction is $X_B X_A$. If each of these probabilities is applied to the value of the field defined by the interaction, i.e., X_A^2 is applied to F_{A-A} , $X_A X_B$ to F_{AB} , and the result summed, then the average field value, F_m , will be obtained. If it is assumed that the A-B interaction is identical to the B-A interaction, then it may be stated that:

$$F_m = X_A^2 F_A^* + 2X_A X_B F_{AB} + X_B^2 F_B^* \quad (24)$$

where

F^* = field value for the pure component.

For the value of the A-B interaction field, F_{AB} , empirical results must be relied upon:

$$F_{AB} = \sqrt{F_A^* F_B^*} \quad (25)$$

For certain systems, it may be necessary to use a three body interaction rather than a two body interaction. The possible interactions then become: AAA, AAB, ABB, BAA, BBA, ABA, BAB, and BBB. In order to simplify matters, it is assumed that F_{AAB} , F_{ABB} , F_{BAA} , F_{BBA} , F_{ABA} and F_{BAB} are all the same as F_{AB} , defined by equation (25). The equation for F_m becomes then:

$$F_m = X_A^3 F_A^* + 3F_{AB}(X_A^2 X_B + X_A X_B^2) + X_B^3 F_B^* \quad (26)$$

Equations (24) and (26) assume that the occurrences of interaction are based on probability alone. This assumption is admittedly questionable. The choice of two body or three body interaction is discussed in Chapter VI, Section 3.

The steps in the prediction of the apparent intermolecular distance are:

- a) From vapor-liquid equilibrium data, G^E is determined.
- b) F_m is predicted from F_A^* and F_B^* (see Sections 5 and 6), and either equation (24) or (26).
- c) L_i is determined from equation (15).
- d) L may then be determined from:

$$L = L_i - \frac{G^E}{NF_m} \quad (27)$$

Thermal conductivity may now be determined by use of equation (12) with the solution properties.

5) The Value of the Pure Component Field

Unfortunately, the values for the pure component fields, F^* , used in equations (24), (25), and (26), are not available and must be determined experimentally. However, once these values have been obtained, they may be used for predicting the solution behavior for any two components that are miscible. This is pointed out and demonstrated in Chapter V, Section 2. The pure component field values may, in theory, be determined exactly, as discussed below.

Although equation (22) is, in general, inexact, it will be noticed that as the solution composition approaches a pure component value, the excess free energy approaches zero, the excess intermolecular distance approaches zero, and the field value approaches the true field value of the pure component. Or it may be stated that:

$$\begin{aligned} \text{As } X &\rightarrow 0 \\ \text{then } L^E &\rightarrow d\bar{S} \\ \text{and } G^E &\rightarrow dW_m \end{aligned}$$

and from equation (20):

$$\bar{F} = \frac{dW_m}{d\bar{S}} = \frac{G^E}{NL^E} \Big|_{X \rightarrow 0} = F^* \quad (28)$$

Thus the extrapolation of the plot of F_m to the pure component compositions yields the value of F^* for that component. Once the value of F^* has been determined for a component, it may be used to predict the apparent intermolecular distance behavior of that component in

solution with another component whose value of F^* is known, as outlined in Section 4.

6) Extension of the Pure Liquid Field Value to Compressibility

If it is assumed that intermolecular forces obey a universal function, such as the Lennard-Jones function, then it may be generalized that the higher the value of the molecular field, the more difficult it will be to move the molecules closer together. Thus a relationship should exist between the molecular field values and the compressibilities of liquids.

Assuming a uniform spherical field around the molecule, the following derivation can be made:

Let:

- r = crude molecular radius, calculated from density, assuming spherical molecules; one-half the center-to-center distance between the molecules.
- Z = the liquid compressibility (reciprocal pressure).
- F = force applied to the molecules to cause compression.

Consider a single column of molecules, stacked one above the other.

The compressibility of this column is given by:

$$Z/\pi r^2 \quad (\text{reciprocal force})$$

Or for the column

$$1/r \frac{dr}{dF} = Z/\pi r^2 \quad (29)$$

$$dF = \frac{\pi r}{Z} dr \quad (30)$$

Assuming Z is constant, equation (30) may be integrated:

$$F = 1.6 \frac{r^2}{Z} + \frac{C_1}{Z} \quad (31)$$

where

$$C_1 = \text{constant of integration}$$

$$FZ = 1.6 r^2 + C_1 \quad (32)$$

F was defined above as the force applied to the molecule to cause compression. This force can be considered proportional to the strength of the molecular field on the assumption stated in the preceding paragraph. Thus:

$$F \propto F^* \quad (33)$$

and equation (32) may be written:

$$(F*Z) = kr^2 + C_2 \quad (34)$$

where

$$k = \text{constant of proportionality}$$

$$C_2 = k C_1$$

Equation (34) predicts a linear relationship between $(F*Z)$ and r^2 , and once the universal constants k and C_2 have been determined, provides a means of predicting F^* for a liquid from its density and compressibility.

7) Applications to Viscosity

In viscous flow, it is necessary to separate the molecules of one layer of liquid from the molecules of the adjacent layer of liquid. Quite obviously, the intermolecular force field plays a part in this process.

First consider the variation of the field with distance as two molecules separate from contact to an infinite separation:

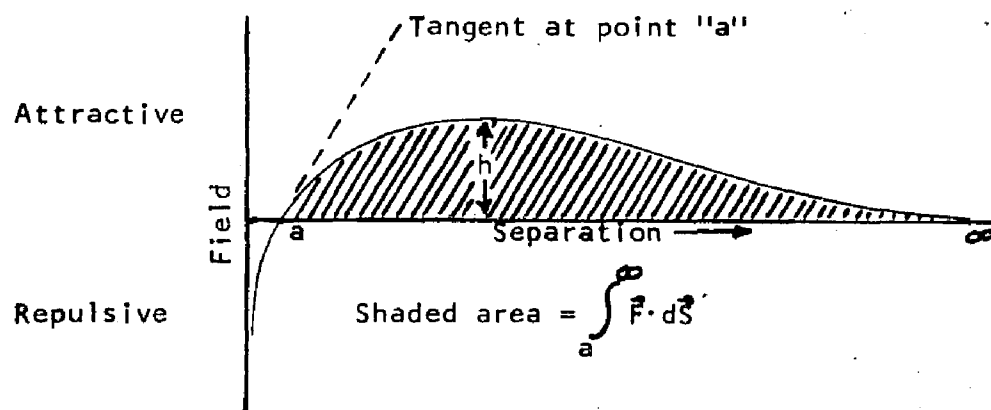


Figure 6

At close approach, there is a strong repulsive field. At point "a", the field changes from repulsive to attractive, the increases in attractiveness and finally drops to zero at infinity. Point "a" is the position of equilibrium at which the travelling molecule experiences no net force. The shaded area represents the work which must be done, and the distance "h" represents the height of the potential hill which must be surmounted, in order to produce a total separation of the molecules. If the function illustrated by Figure 6 is considered to be a universal

function, as in Section 6, then the slope of the curve at point "a" is indicative of the height "h" and the work of separation. Thus:

$$\int_a^{\infty} \vec{F} \cdot d\vec{S} = f \left(\frac{dF}{dL_{cc}} \right)_a \quad (35)$$

where

L_{cc} = the center-to-center distance between molecules.

Since the slope at "a" represents the work to be done in separating molecules, as must be done in viscous flow, viscosity should be a function of this slope.

Since viscosity concerns a shear stress, it is necessary to apply a correction to the value of viscosity expressed on a unit area basis to bring it to a uni-molecular area basis if it is to be correlated with molecular forces. Thus from the definition of viscosity:

$$\tau = \mu \frac{du}{dy} \quad (36)$$

where

τ = shear stress, unit area basis

μ = viscosity, force time/area

$\frac{du}{dy}$ = velocity gradient in the fluid

the correction can be made:

$$\frac{\tau \pi p^2}{\left(\frac{du}{dy} \right)} = \mu \pi p^2 \quad (37)$$

For convenience let

$$m = \left(\frac{dF}{dL_{cc}} \right)_a \quad (38)$$

Then the expected relationship is:

$$r^2 = f(m) \quad (39)$$

"m" may be determined for the pure liquid in the following manner.

First a plot of F_m versus molar composition is made, and is differentiated graphically at the pure component composition, as illustrated in Figure 7:

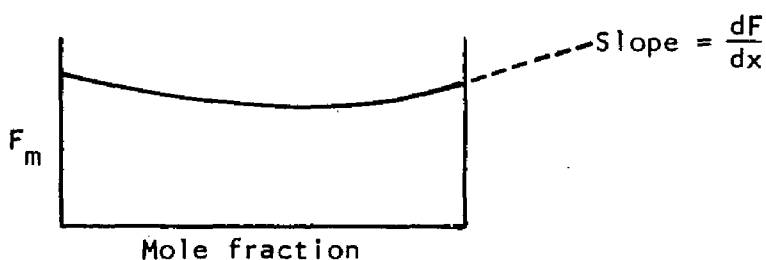


Figure 7

This yields $\frac{dF}{dX}$ at the pure component composition. A similar plot is made for L_{cc} versus composition, and it too is differentiated graphically at the pure component composition; yielding $\frac{dL_{cc}}{dX}$. "m" is then given by:

$$m = \frac{dF}{dX} \frac{dX}{dL_{cc}} \quad (40)$$

L_{cc} of equation (40) is defined by:

$$L_{cc} = (X_1 d_1 + X_2 d_2 + L) \quad (41)$$

where

$d = (L_{cc} - L)$ for the pure component. L_{cc} for the pure component is determined from density assuming spherical molecules. "d" represents the diameter of the "hard" molecule.

8) Relationship Between Viscosity and Compressibility

Equation (29) may be restated as:

$$\frac{r}{Z} = f(m) \quad (42)$$

This may be compared with equation (39):

$$\mu r^2 = f(m) \quad (39)$$

Thus it would be expected that

$$\mu r^2 = f \frac{r}{Z} \quad (43)$$

A discussion of this relationship appears in Chapter VI, Section 6.

9) Theory Recapitulated

In Section 6, the relationship of compressibility to molecular field was derived and presented as a possible means for predicting F^* , the pure liquid molecular field value.

Section 5 presented the method of using the pure component field values, together with vapor-liquid equilibrium data, to obtain the apparent intermolecular distance of the solution at any given composition. This in turn may be used to calculate the thermal

conductivity of the solution. It is to be noted that the method of Section 6 is entirely independent of the method of Section 5.

Section 7 made further use of the molecular field concept by relating it to viscosity.

Section 8 related viscosity to compressibility through the common parameter, "m".

CHAPTER III

APPARATUS

The quantity measured experimentally in this investigation was thermal conductivity. The apparatus used was designed by Sakiadis and Coates, and was thoroughly tested in previous projects.²¹

The apparatus is shown in Figure 8. Photographs of the installation are presented in Figures 9 through 15.

The apparatus consists of a hot bar and a cold bar mounted vertically within a pyrex glass pipe, with the hot bar uppermost. The liquid sample is placed between the two bars. The glass pipe permits visual observation of the liquid film, which is necessary for removing bubbles. The height of the hot bar may be adjusted to give any desired liquid film thickness to 0.9599 ± 0.0005 in. Temperatures within the bars are measured by thermocouples. The bars are maintained at their temperatures by circulating water from constant temperature baths. The terms hot and cold are relative only. The hot bar may actually be near room temperature.

The hot bar, 5.731 in. in diameter and 1.25 in. long, is constructed of nickel plated steel. The bar is attached to a short section of steel pipe of the same diameter, which in turn is bolted to a steel plate. The bar, pipe, and plate form a chamber through which the hot water is circulated. The hot water is fed into and removed from

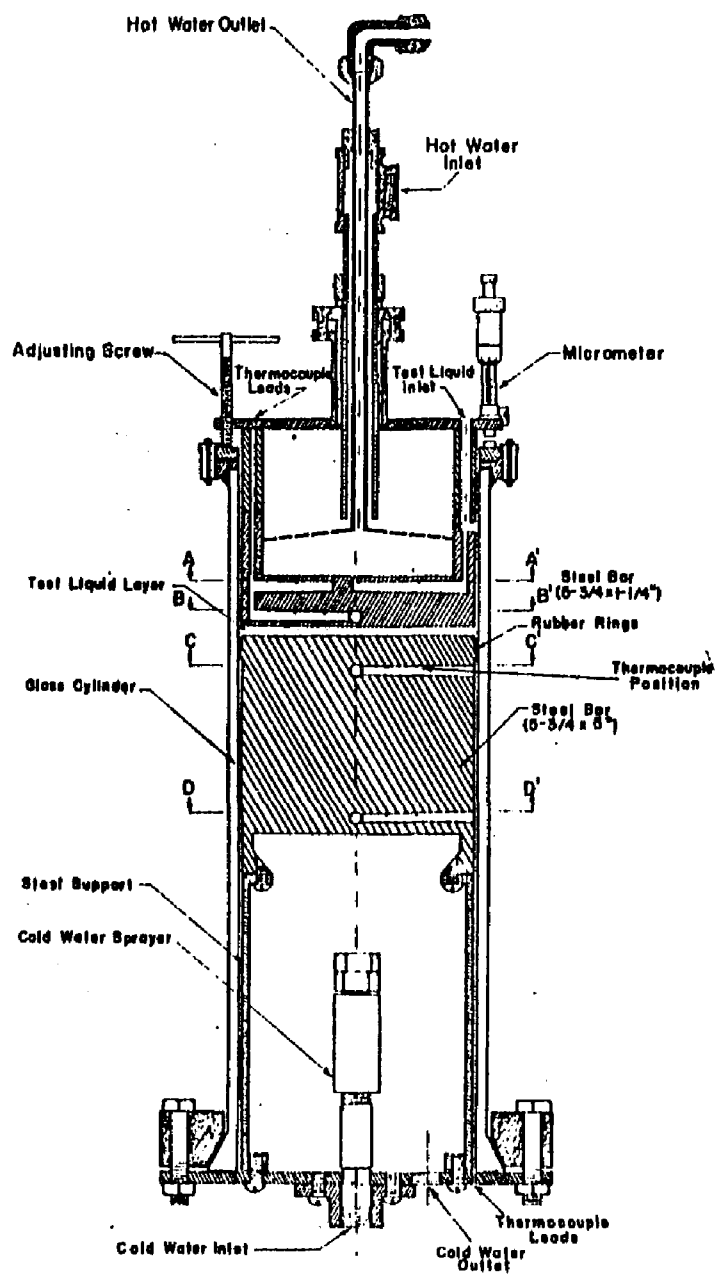
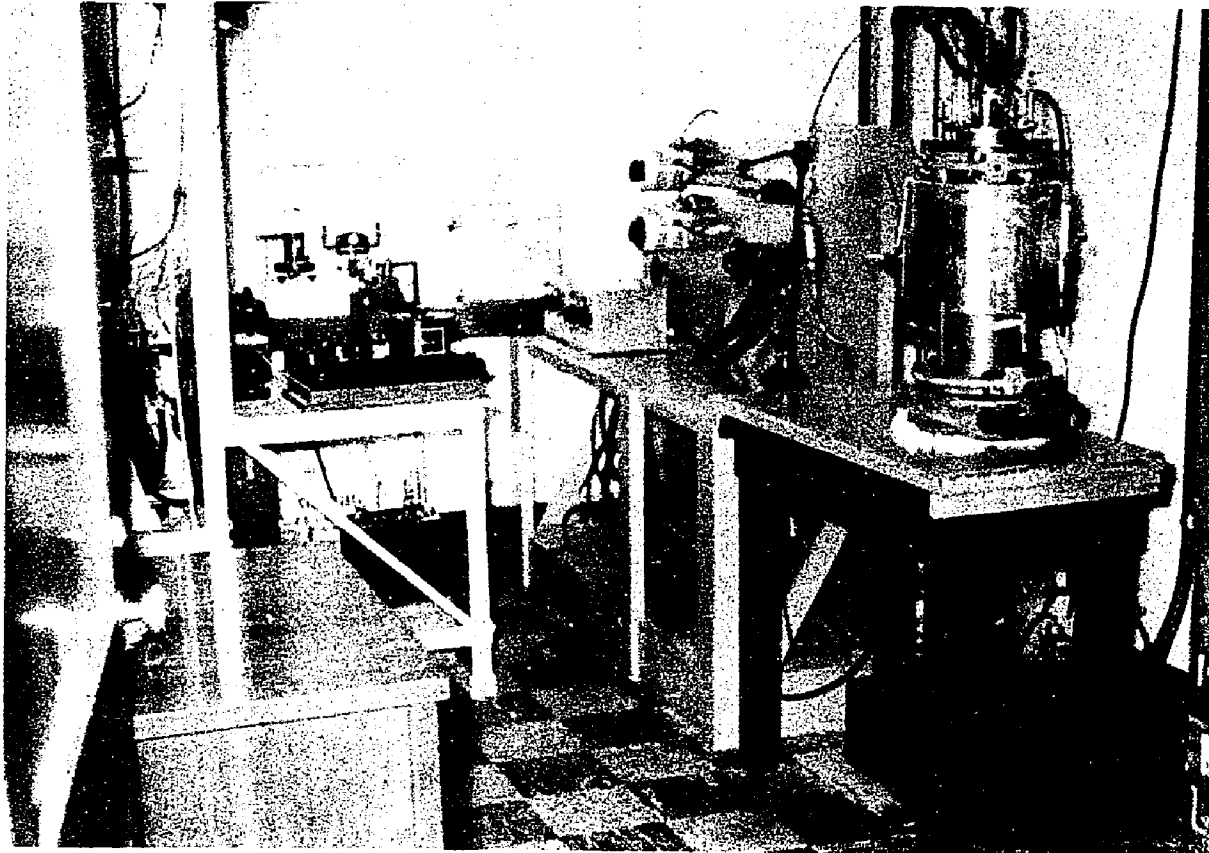
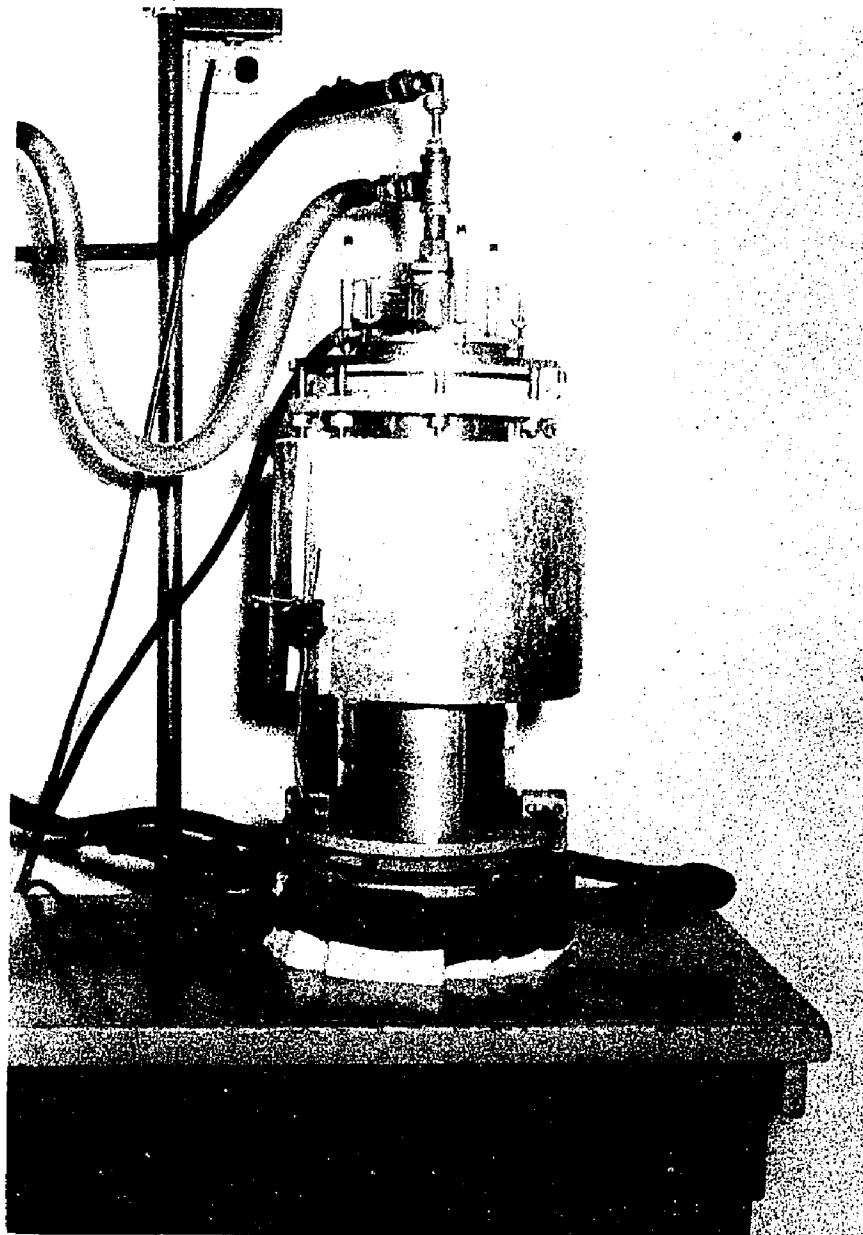


FIGURE 8
THERMOCONDUCTIMETRIC APPARATUS
FOR LIQUIDS



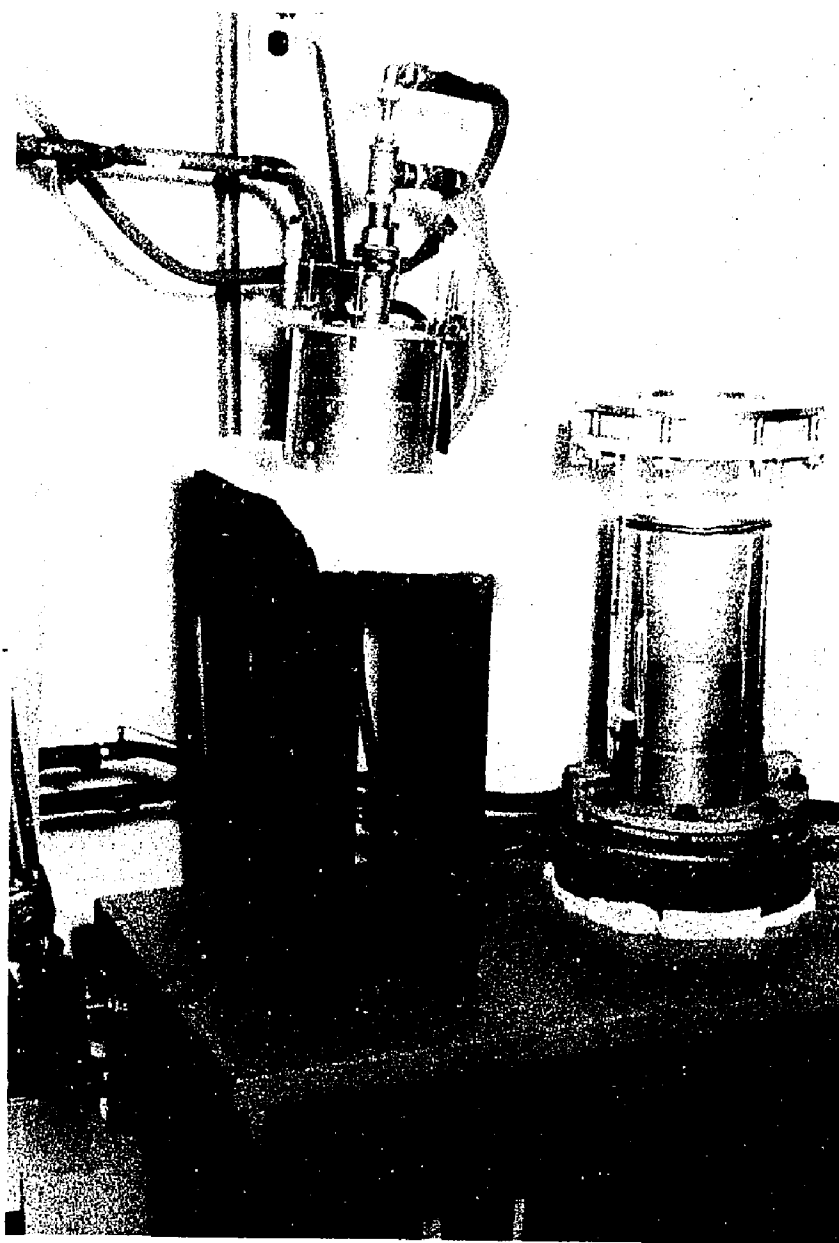
General View

Figure 9



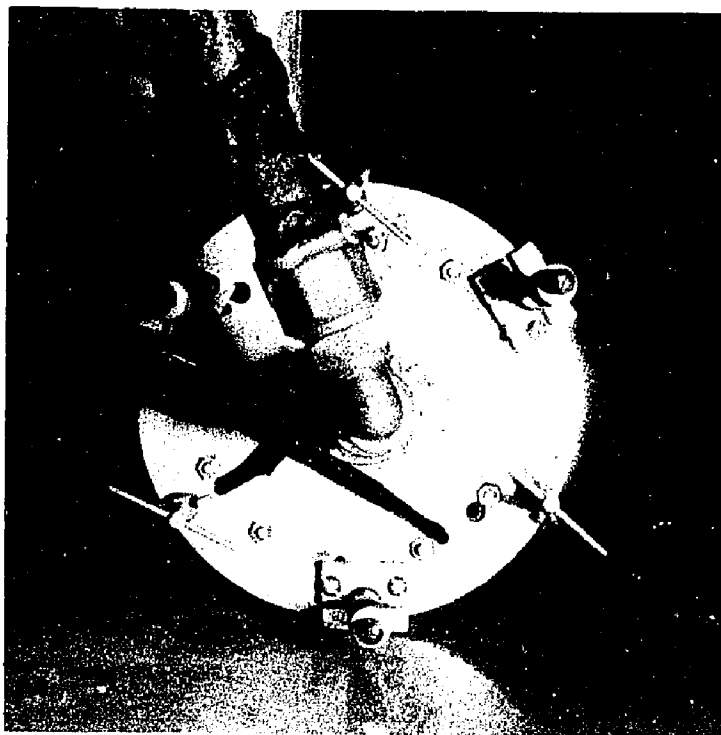
Apparatus In Operation

Figure 10



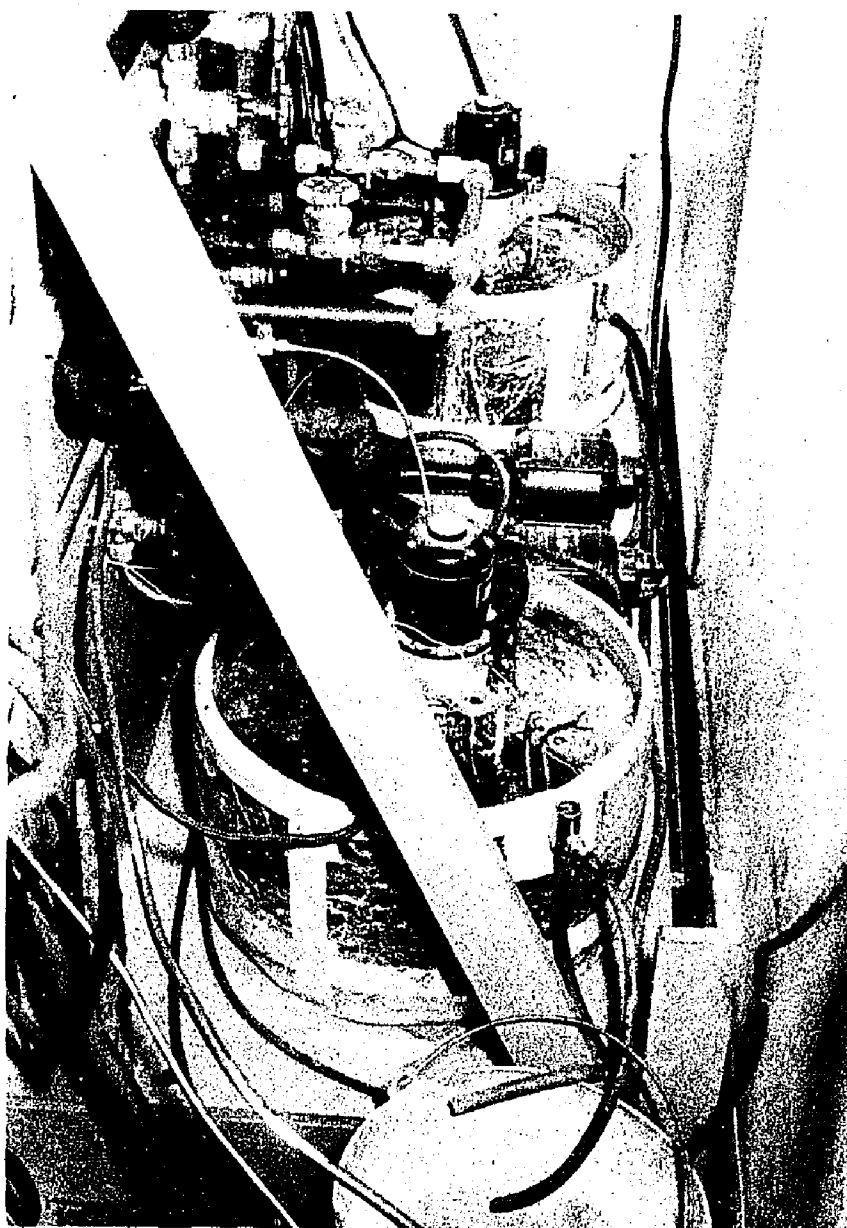
Apparatus Disassembled

Figure 11



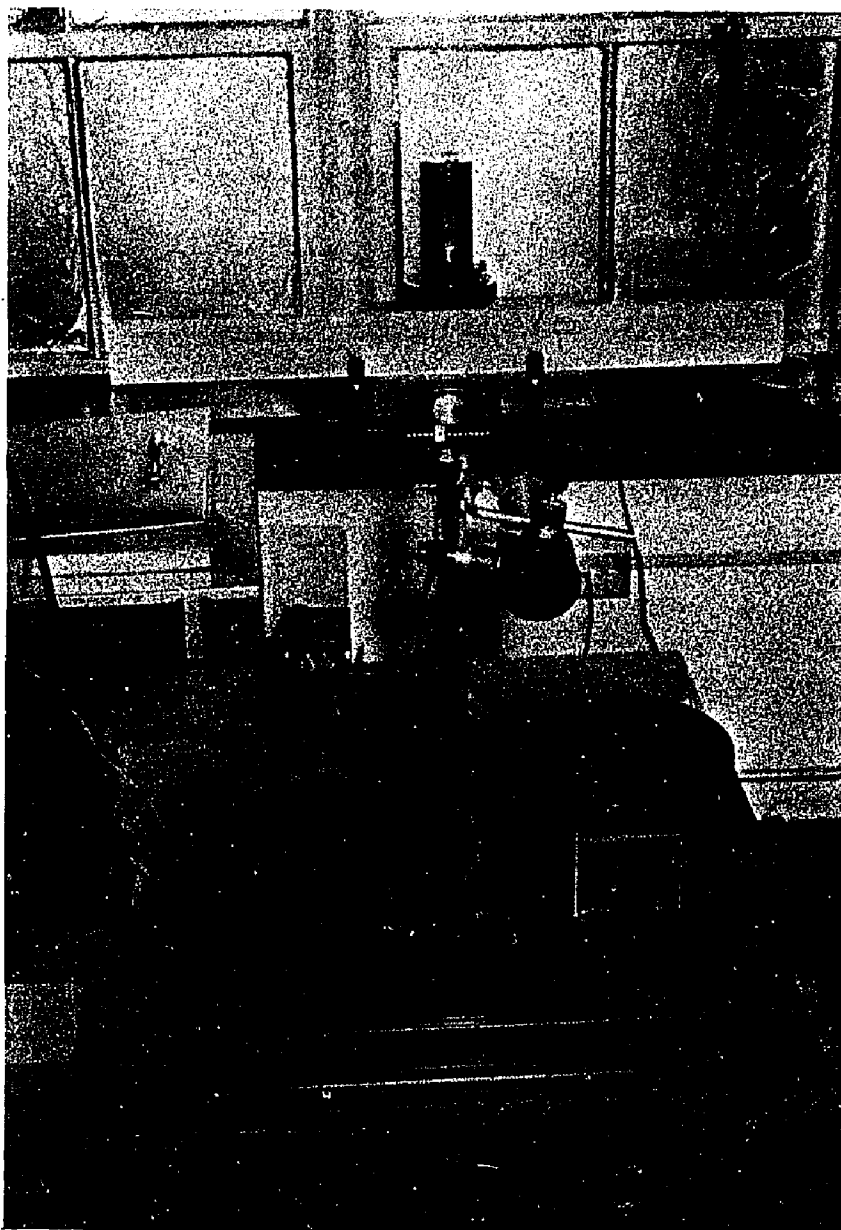
Top View of the Hot Bar

Figure 12



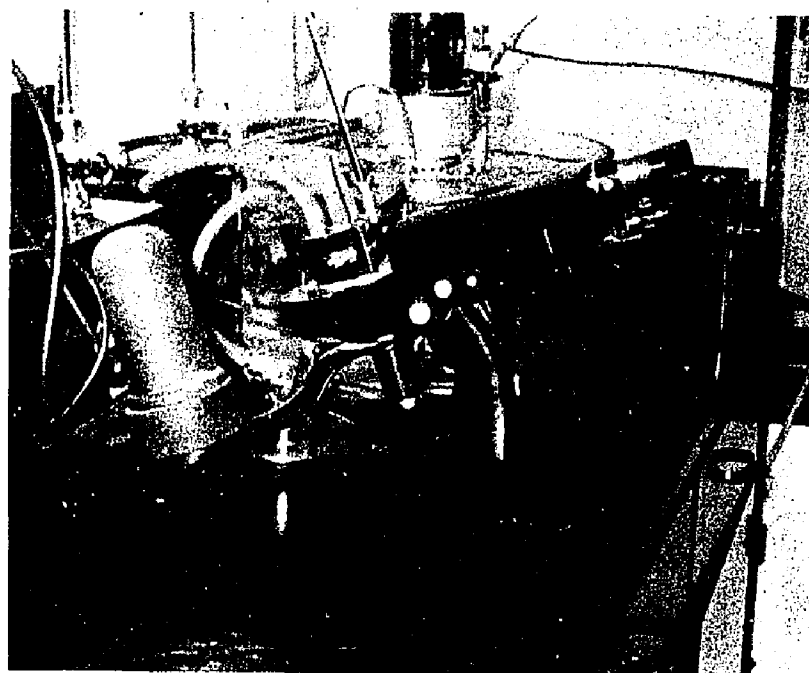
Water Baths

Figure 13



Potentiometer and Galvanometer

Figure 14



Refractometer

Figure 15

the chamber through two concentric pipes. The water enters through the center pipe, circulates within the chamber and leaves through the annular space formed by the outer pipe. To prevent short circuiting of the water, the chamber is fitted with a water distributor, attached to the inlet pipe. Five thermocouples are embedded in taper pins which are driven into the hot bar. The distance from the thermocouple plane to the surface of the hot bar is 0.400 in.

The plate to which the hot bar is attached is equipped with three jack screws and three micrometers spaced alternately, 60° apart (Fig. 12). The screws bear upon a steel ring which is clamped to the flare of the pyrex pipe. The screws are used to adjust the height of the hot bar above the cold bar, which adjusts the liquid film thickness. The micrometers are used to measure the film thickness by the difference in readings obtained with the hot bar up and with the hot bar resting on the cold bar.

The cold bar, 5.731 in. in diameter and 5.000 in. long, was machined from the same steel shaft as the hot bar. The cold bar is attached to a length of steel pipe of the same diameter. The pipe is closed by a steel plate, forming the cold water chamber. A spray nozzle is fitted into the chamber to distribute the cold water over the bottom of the bar. The water leaves the chamber through an outlet in the plate. Ten thermocouples are mounted in two layers in the cold bar as shown by Fig. 8. The middle layer of thermocouples is 0.73 in. from the surface at the cold bar. The thermocouple layers in the cold bar are 3.7432 in. apart.

The pyrex pipe is clamped to the plate of the cold bar. The annular space between the cold bar and the glass pipe is sealed by two rubber "O" rings near the top of the cold bar. The annulus formed by the hot bar and the pyrex pipe is sealed by a third "O" ring which may be slid down to close the opening after the thickness is set.

Liquid is introduced into the apparatus through either of two 1/4 in. holes drilled from the plate of the hot bar to the annular space between the hot bar and the pyrex pipe.

The thermocouples of each layer (B, C, D) are connected in parallel to give an average temperature of the layer. Thermocouple emf is measured by a Type K-2 Leeds and Northrup potentiometer using a Type A Leeds and Northrup galvanometer (Figure 14). The thermocouple reference junctions are maintained at the ice point by an ice bath in a Dewar flask.

To eliminate heat losses from the cold bar an electrically heated jacket is placed around the pyrex pipe (Figure 10). Three thermocouples are mounted on the pyrex pipe, one opposite layer C, one opposite D, and one between C and D. The current to the jacket is adjusted using a powerstat so that there is no net heat lost or gained by the cold bar as determined by the thermocouples on the pipe.

The water baths (Figure 13) are equipped with American Instrument Company thermoregulators and Sargent relays, which control the water temperature to $\pm 0.005^{\circ}\text{F}$. The cold bath can be refrigerated if necessary.

Two centrifugal pumps circulate the hot and the cold water.

The discharges of the pumps are connected to the apparatus by flexible rubber tubing rather than by metal pipe to eliminate pump vibration.

To further reduce vibrations, the bars and supports are mounted on foam rubber on a heavy table separate from the platform supporting the pumps and water baths (Figure 9).

Solution composition is determined by means of the refractive index at 25°C. A Bausch and Lomb refractometer equipped with a Sargent constant temperature bath is used for the refractive index determinations (Figure 15).

CHAPTER IV

PROCEDURE

- 1) Adjust the thermoregulators to give the desired temperatures of the water baths.
- 2) Turn on the thermoregulator relays, heating elements, and refrigerator, and allow the baths to reach the desired temperatures.
- 3) Turn on the water circulating pumps to bring the bars to the desired temperatures.
- 4) Pour 100 ml. of freshly boiled liquid into the apparatus.
- 5) Lower the hot bar until it rests on the cold bar, and take micrometer readings.
- 7) Raise the hot bar until the desired liquid film thickness is obtained as determined by the micrometers, and then slide the sealing gasket down.
- 8) Place the jacket around the pyrex pipe and adjust the powerstat to an approximate setting.
- 9) Allow thirty minutes for the apparatus to approach equilibrium.
- 10) Lower the hot bar rapidly until it rests on the cold bar and take micrometer readings.
- 11) Raise the hot bar and adjust the liquid film thickness and gasket as in Step 7.

- 12) Allow one hour for the apparatus to reach equilibrium. During this time, adjust the jacket powerstat so that there is no net heat lost or gained by the cold bar. This condition is attained when the algebraic sum of the differences between the jacket thermocouples and their respective layers is less than 20 microvolts.
- 13) Begin thermocouple readings. When three consecutive readings of each layer agree to within 0.5 microvolt over a period of one-half hour, the run is complete.
- 14) Take micrometer readings with the hot bar up.
- 15) Lower the hot bar rapidly until it rests on the cold bar and take micrometer readings. The average difference in micrometer readings obtained in (14) and (15) is the film thickness to be used in the calculations.
- 16) Remove the hot bar and withdraw a sample for analysis.

For successive runs at the same water bath temperatures, the height of the hot bar may be set by using the micrometer readings obtained with the hot bar down in the preceding run. This gives more consistent film thicknesses, and eliminates Steps 6, 9, 10, and 11.

CHAPTER V

RESULTS

1) Determination of the Molecular Field Values

The effective intermolecular distances, as defined in Section 2 of Chapter II, were determined as functions of composition for eleven binary liquid mixtures at 25°C and 1 atmosphere, using equation (12) and literature data.^{1, 3, 12, 14, 21} These values are plotted in Figures 16 through 18.

From the values of intermolecular distance, values of the excess intermolecular distance, L^E , defined in connection with equation (22), were determined, using the ideal intermolecular distance defined by equation (15). These values of the excess intermolecular distance are plotted in Figures 19 through 21.

Excess free energy values, G^E , were determined for the same eleven systems using equation (23) and vapor-liquid equilibrium data taken from the literature.² These values are plotted in Figures 22 through 24.

From the values of L^E and G^E , the average molecular field, F_m , was determined as a function of composition, using equation (22), for six of the eleven systems. The other five of the eleven systems did not exhibit sufficient deviation from ideal behavior to

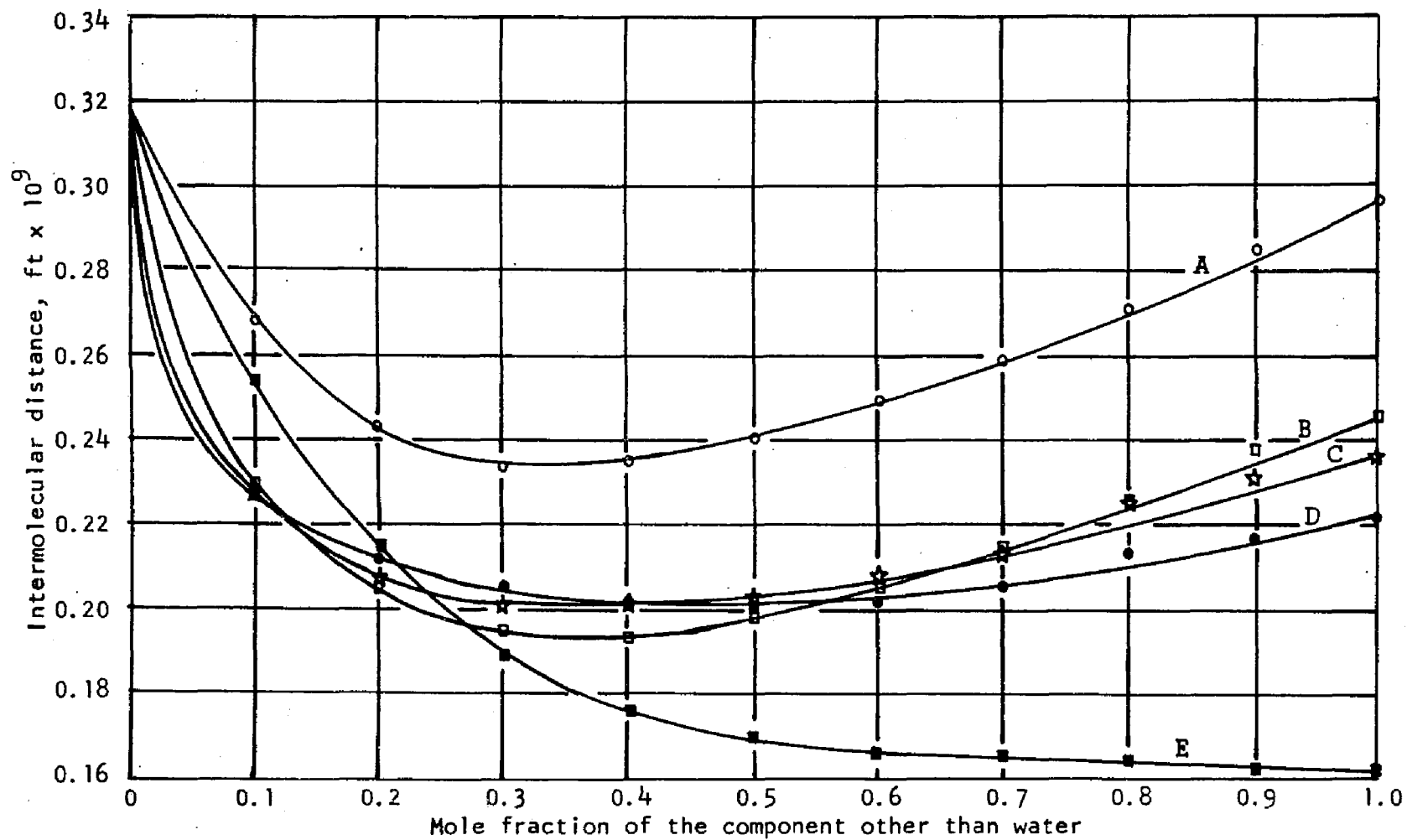


Figure 16. Intermolecular Distance versus Composition for Aqueous Solutions. Non-aqueous components are: for curve A - methanol, B - acetone, C - ethanol, D - propanol(n), and E - glycerine.

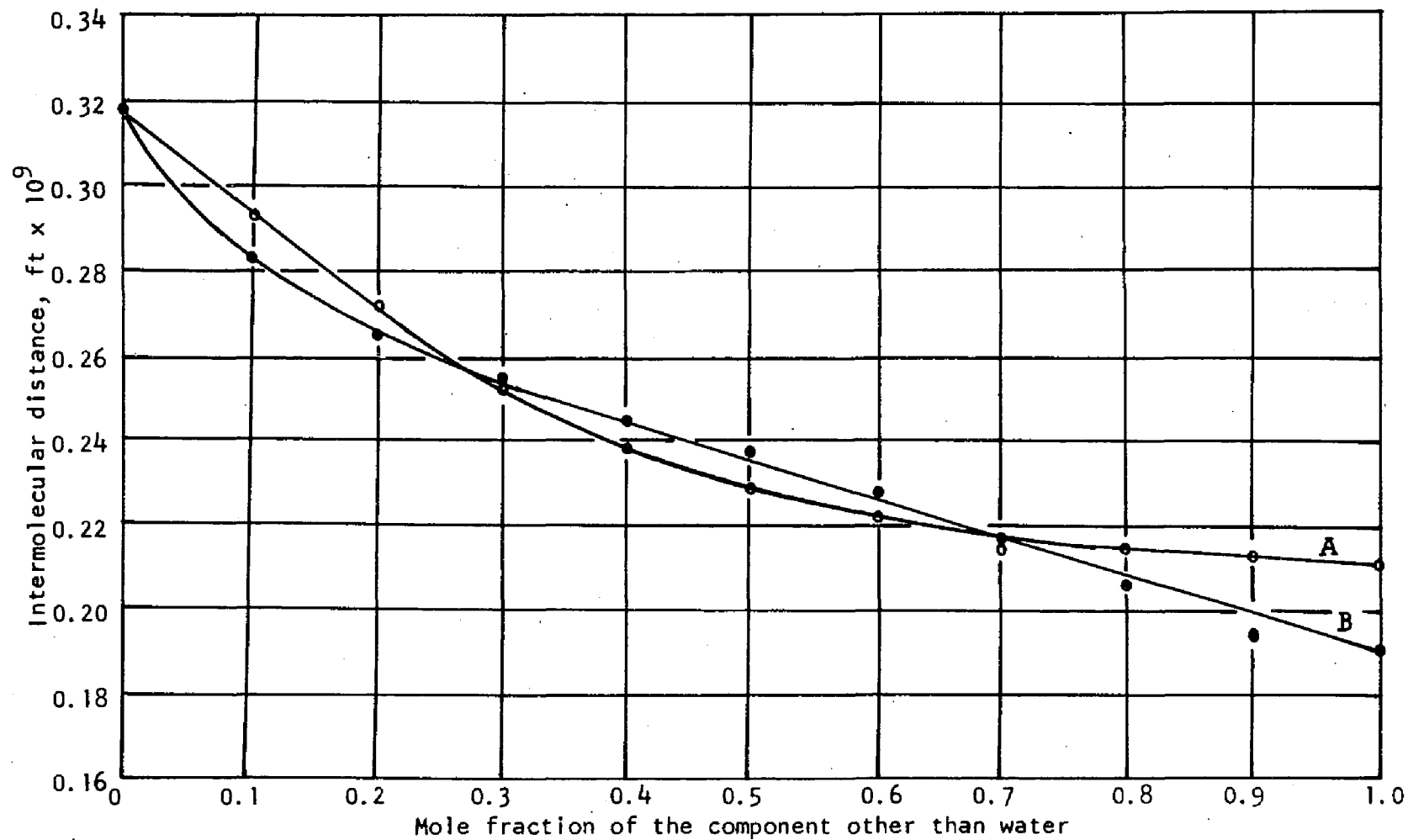


Figure 17. Intermolecular Distance versus Composition for Aqueous Solutions. Non-aqueous components are: for curve A - acetic acid, and for B - ethylene glycol.

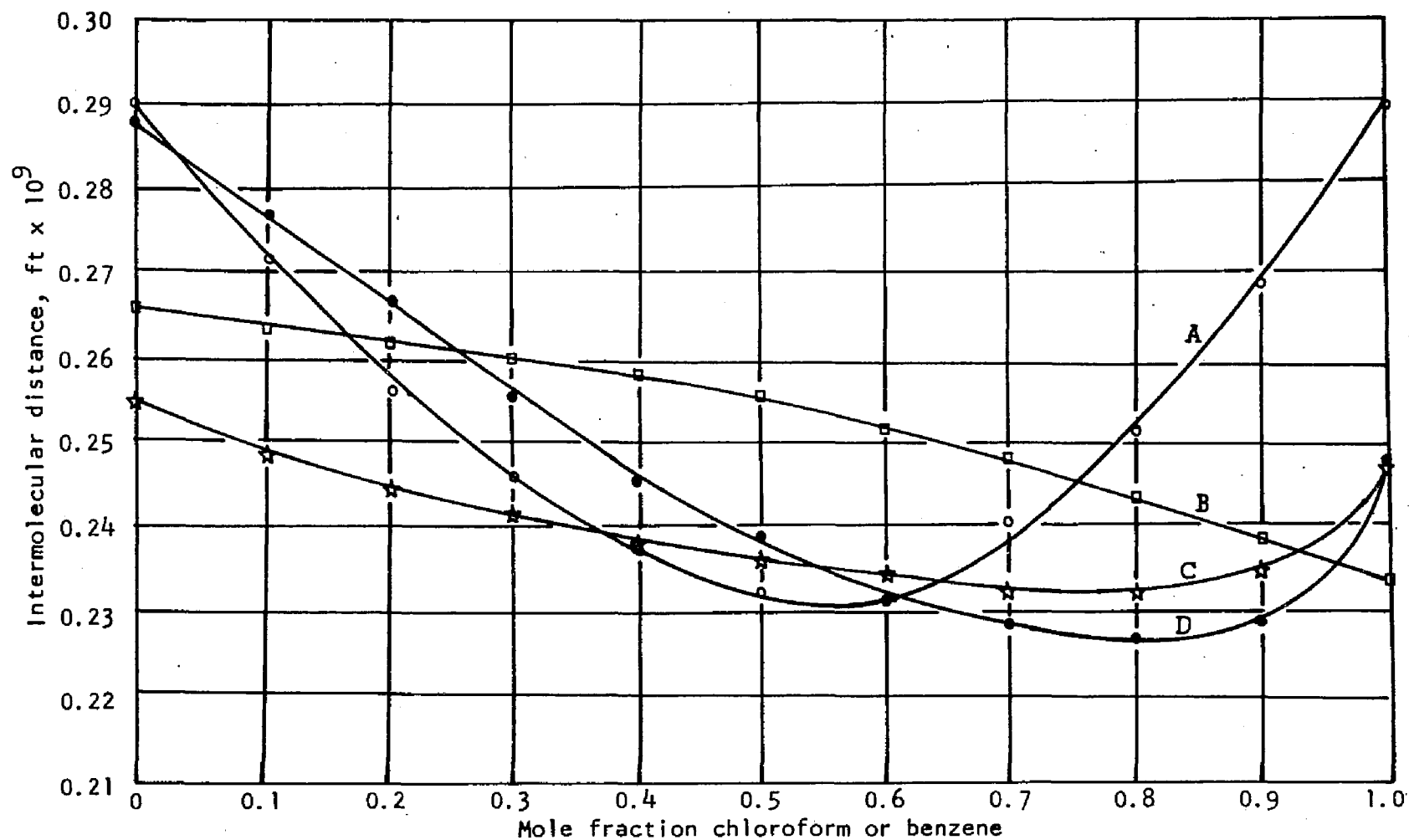


Figure 18. Intermolecular Distance versus Composition for Organic Solutions. The solutions are: for curve A - ethyl ether + chloroform, B - acetone + benzene, C - carbon tetrachloride + benzene, and D - ethyl ether + benzene.

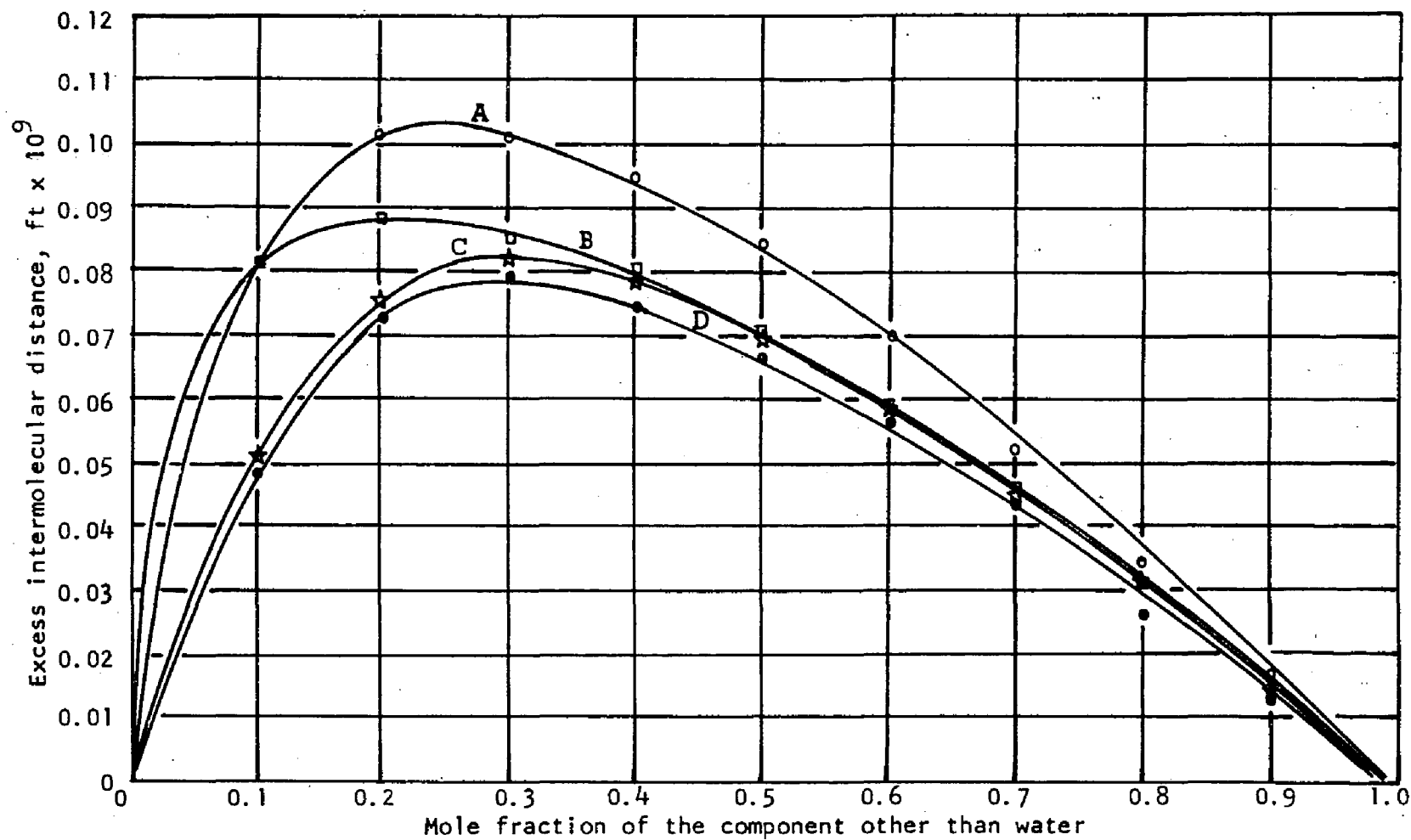


Figure 19. Excess Intermolecular Distance versus Composition for Aqueous Solutions. Non-aqueous components are: for curve A - acetone, B - propanol(n), C - glycerine, and D - methanol.

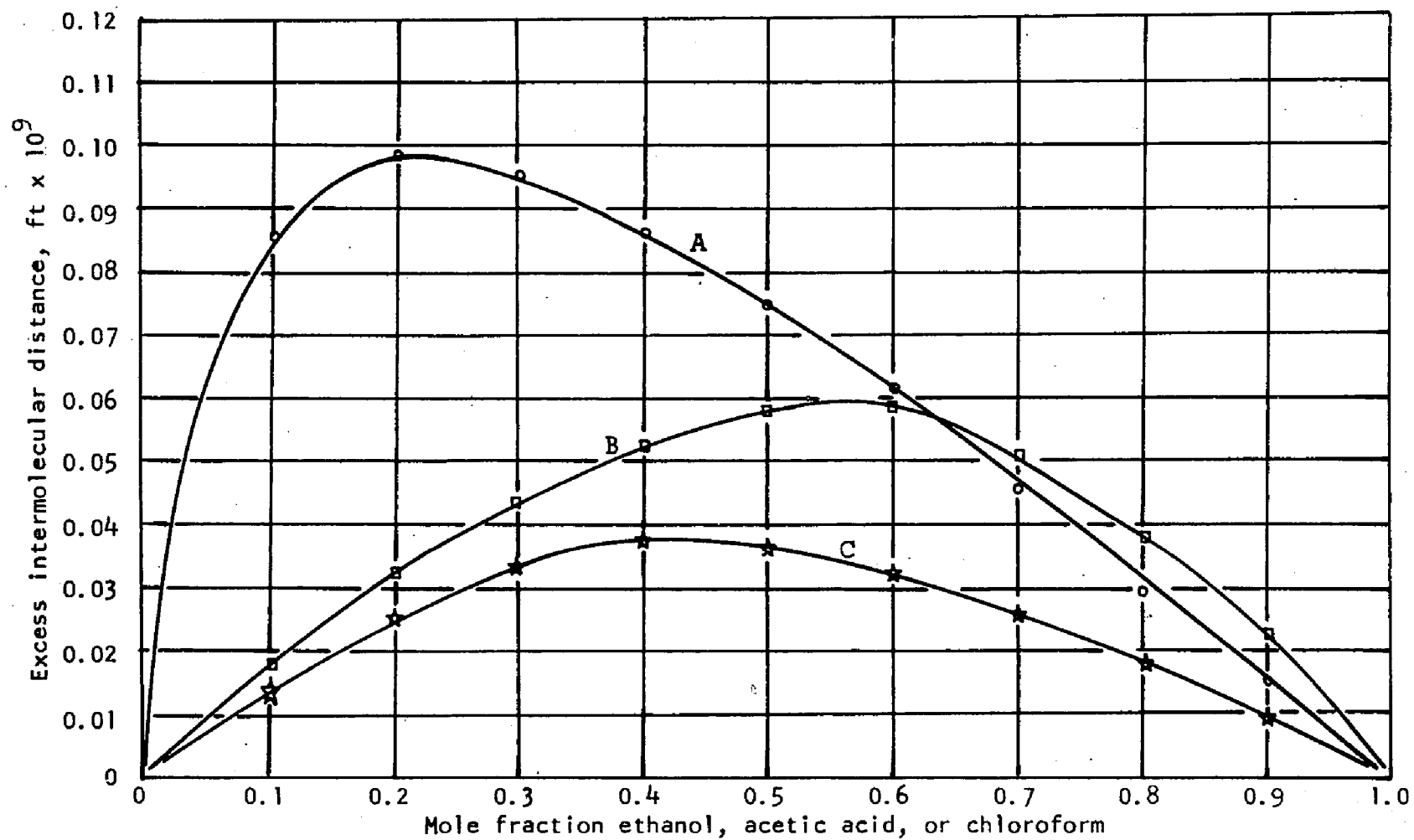


Figure 20. Excess Intermolecular Distance versus Composition. The solutions are: for curve A - ethanol + water, B - ethyl ether + chloroform, C - acetic acid + water.

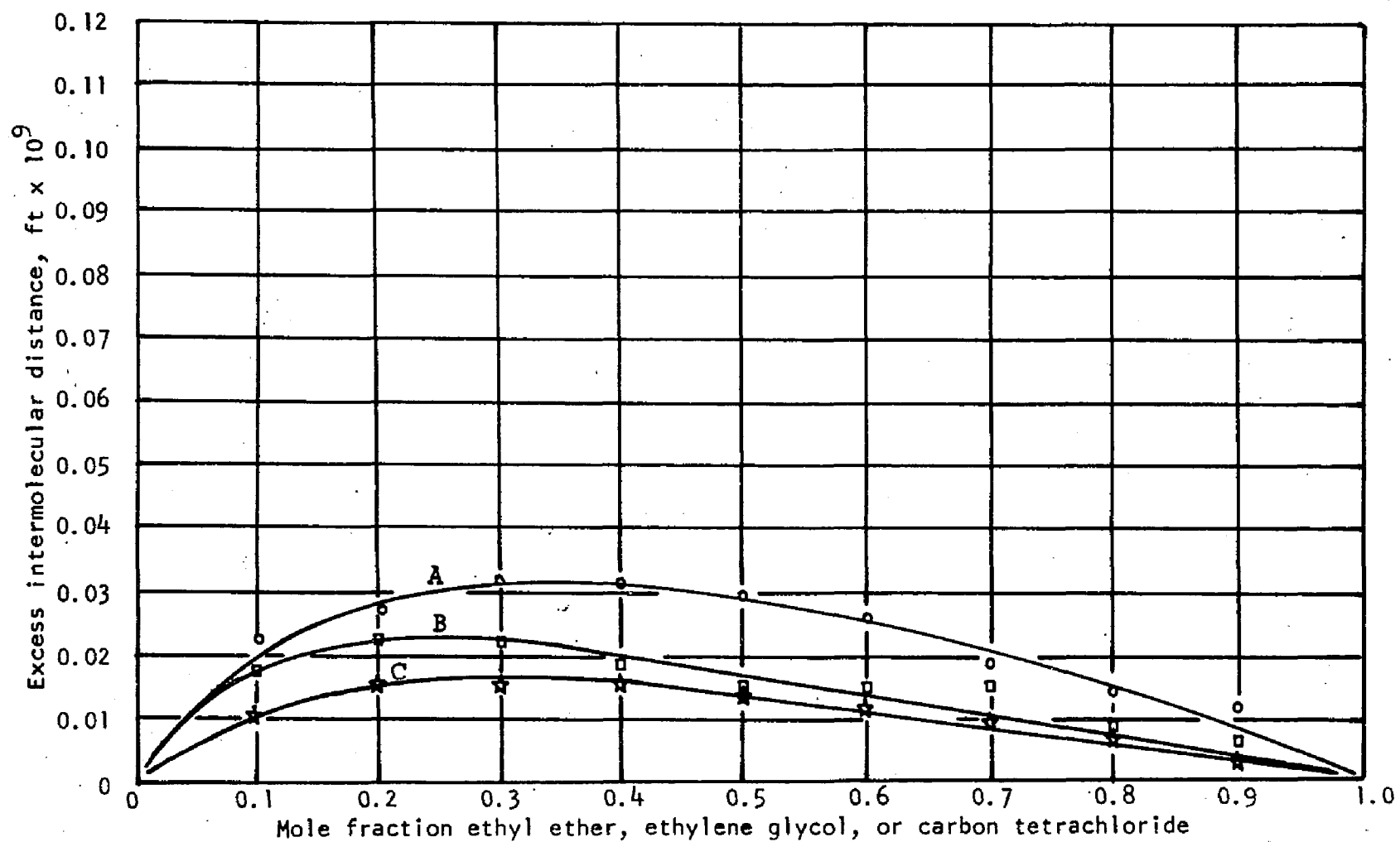


Figure 21. Excess Intermolecular Distance versus Composition. The solutions are: for curve A - ethyl ether + benzene, B - ethylene glycol + water, and C - carbon tetrachloride + benzene.

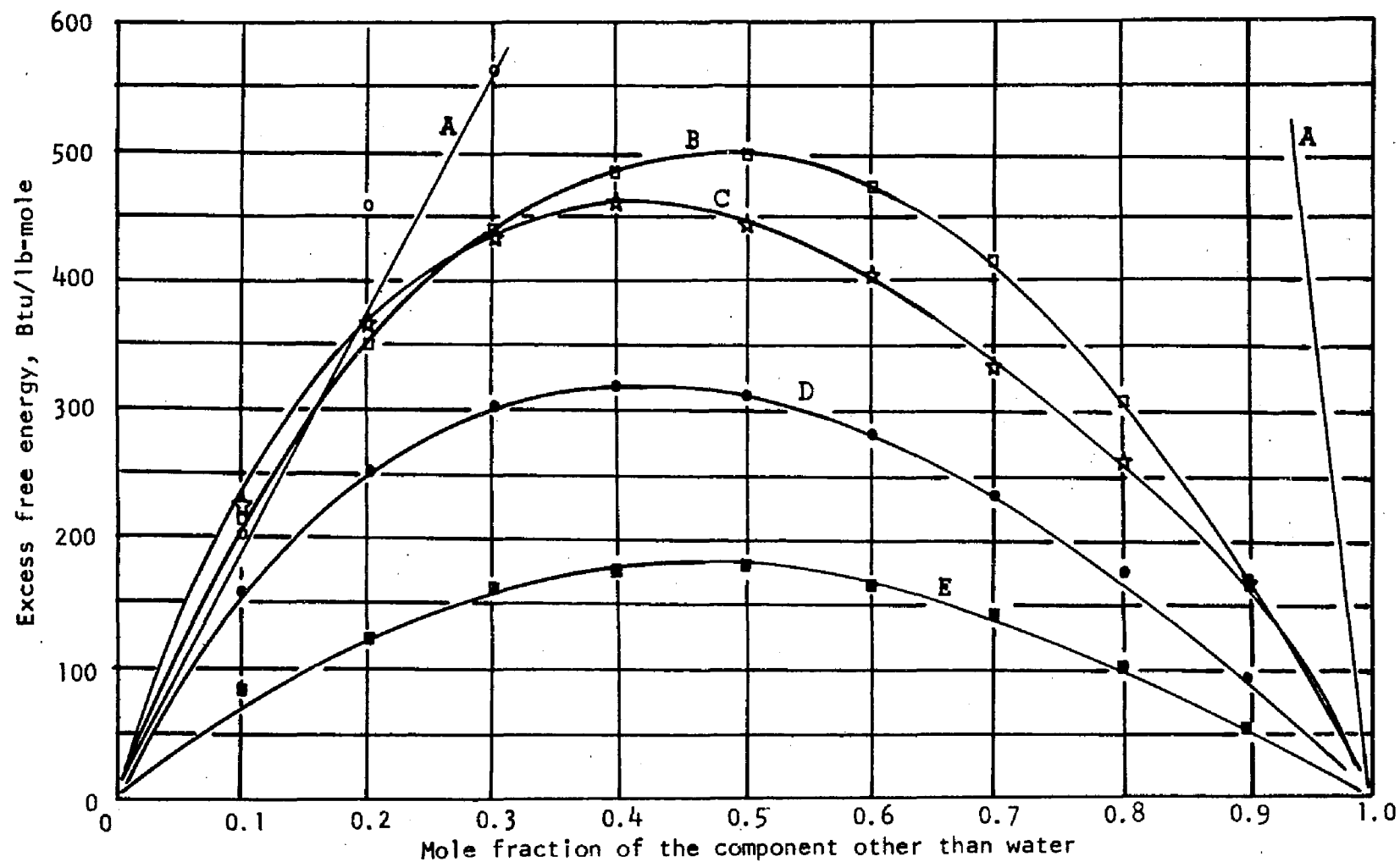


Figure 22. Excess Free Energy versus Composition for Aqueous Solutions. Non-aqueous components are: for curve A - glycerine, B - acetone, C - propanol(n), D - ethanol, E - methanol. Curve A appears in Figure 23 on a reduced scale.

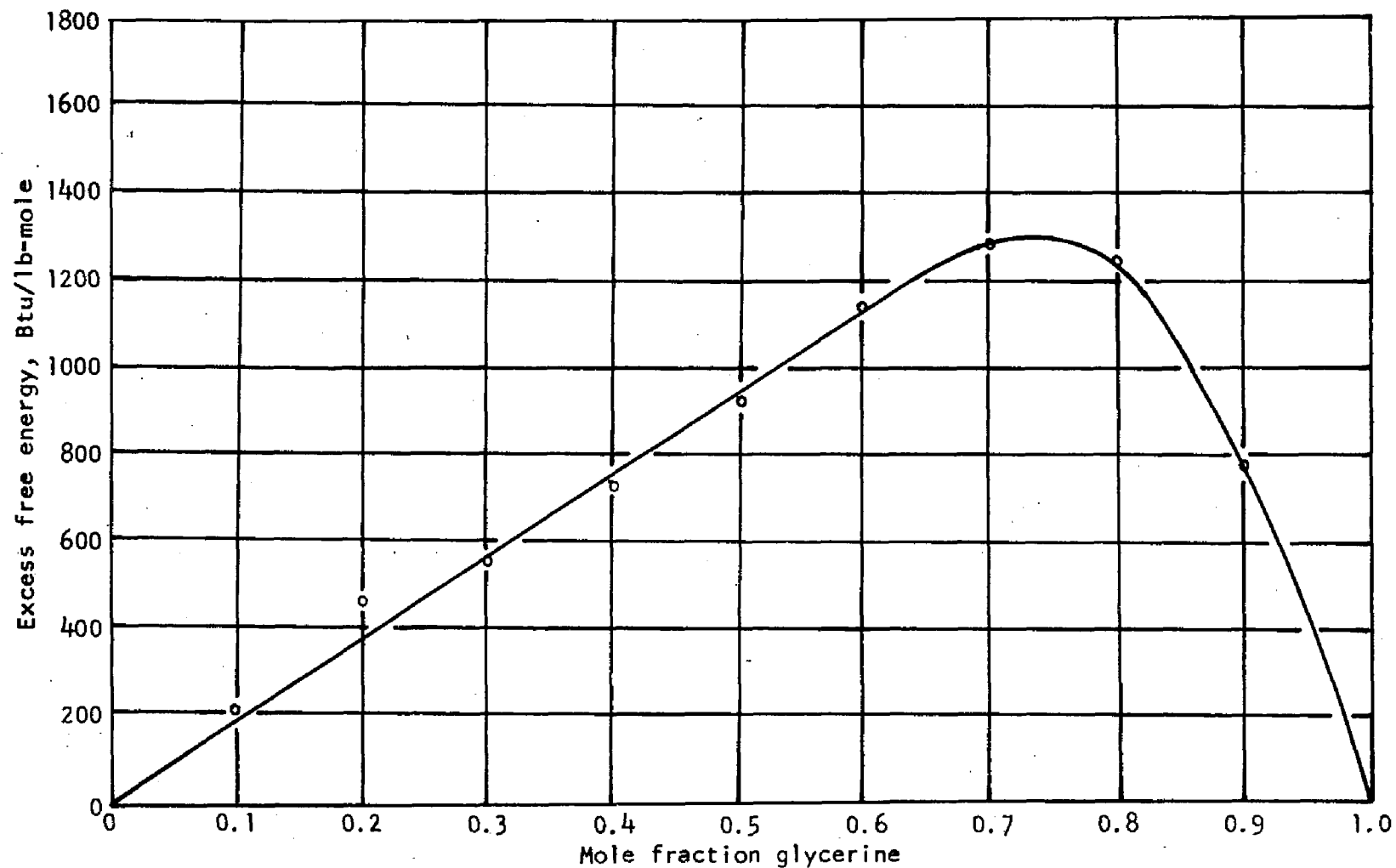


Figure 23. Excess Free Energy versus Composition for the Glycerine + Water System. Note the change of scale from Figure 22.

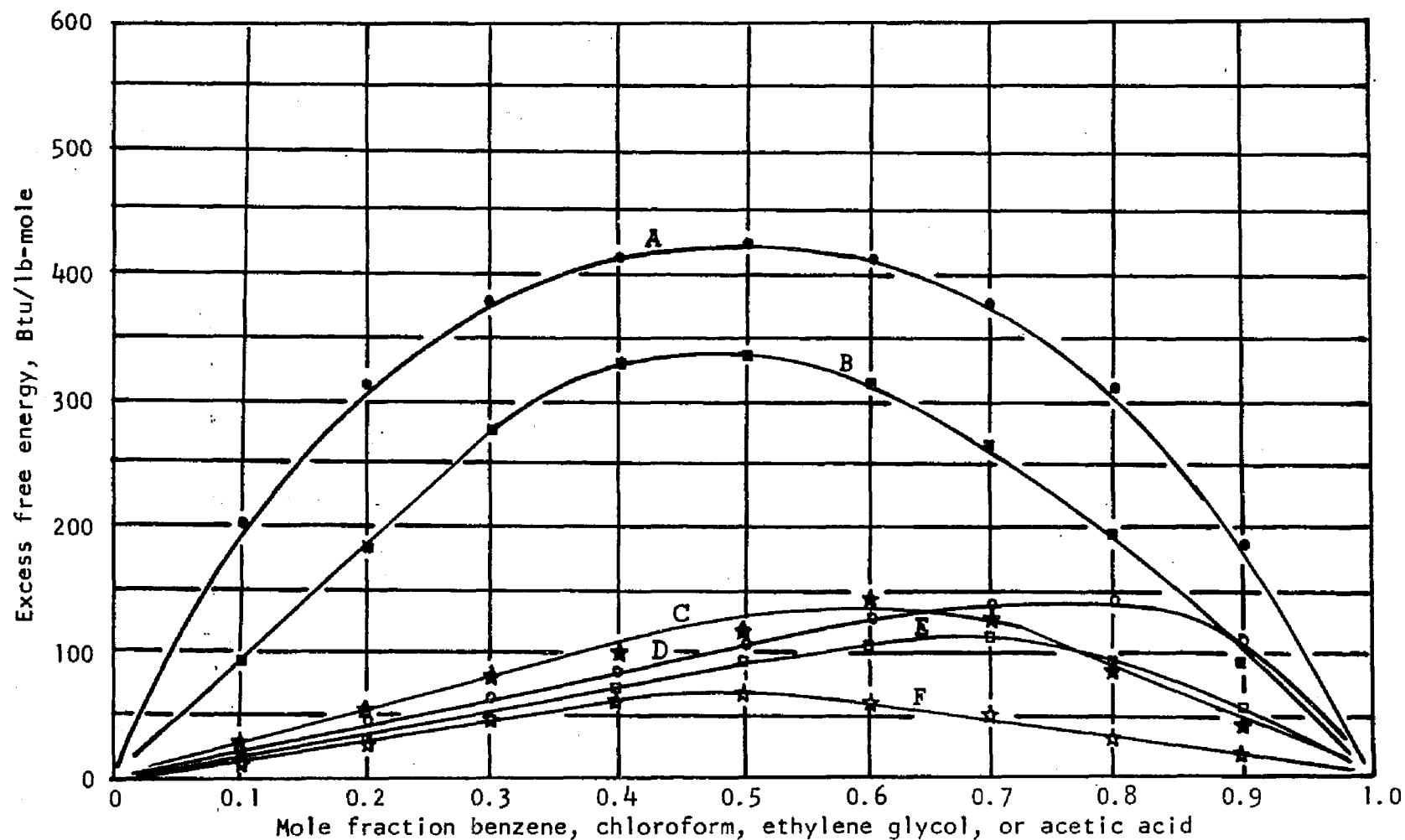


Figure 24. Excess Free Energy versus Composition. The solutions are: for curve A - ethyl ether + benzene, B - ethyl ether + chloroform, C - water + ethylene glycol, D - carbon tetrachloride + benzene, E - water + acetic acid, and F - acetone + benzene. For curves B, C, and D, the excess free energy is negative.

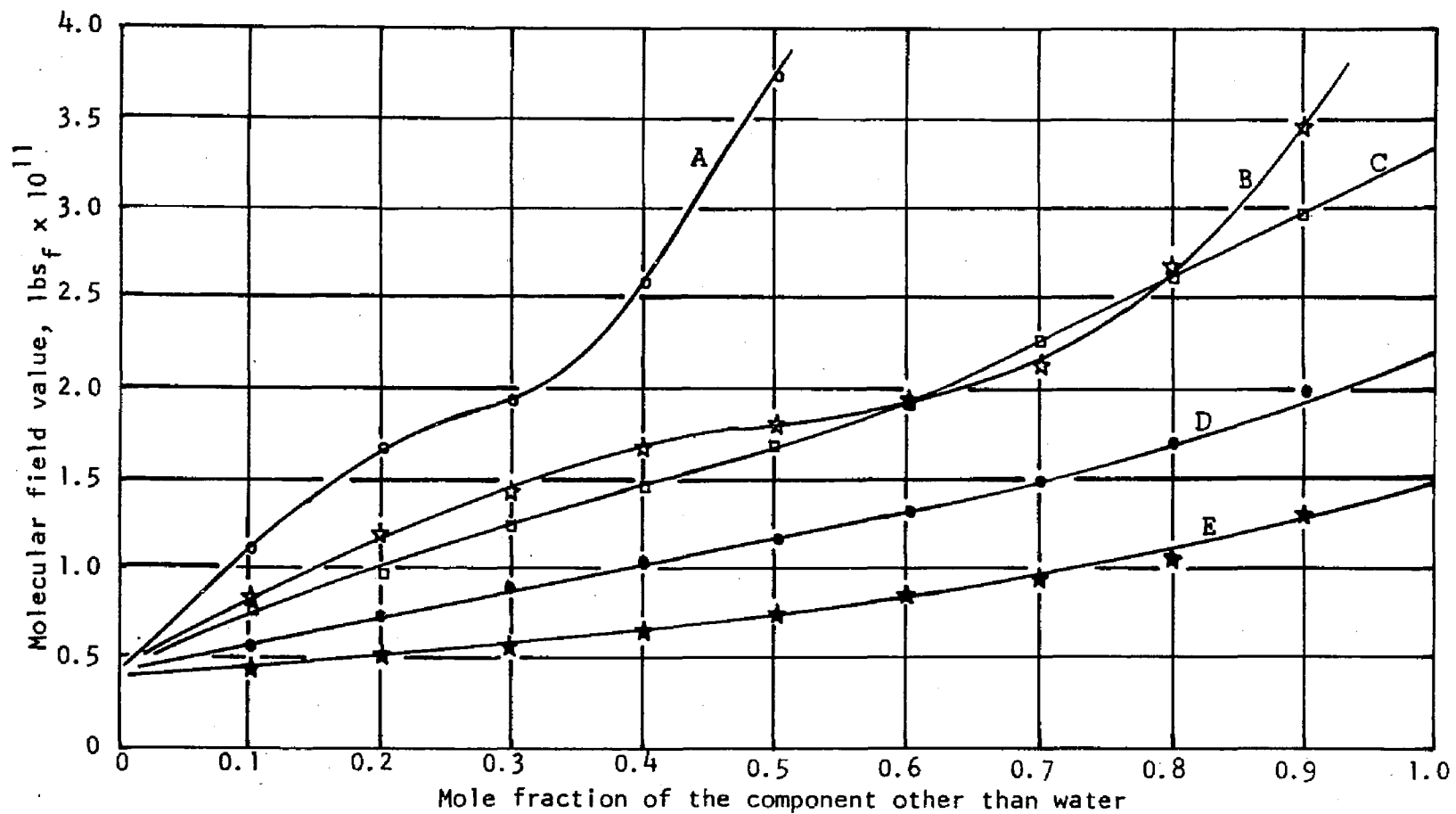


Figure 25. Molecular Field Value versus Composition for Aqueous Solutions. Non-aqueous components are: for curve A - glycerine, B - propanol(n), C - acetone, D - ethanol, and E - methanol. Curves A and B appear in Figure 26 on a reduced scale.

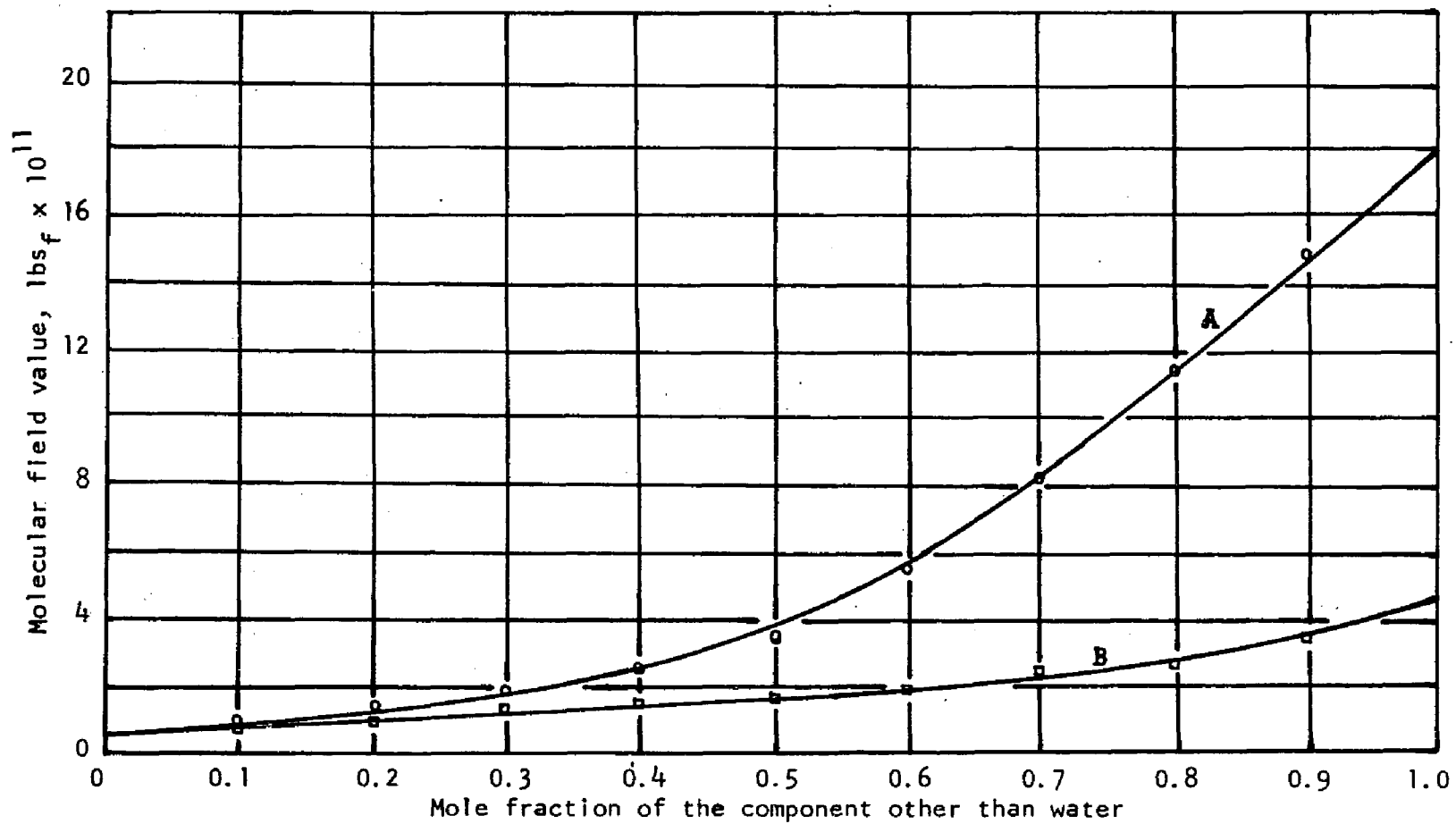


Figure 26. Molecular Field Value versus Composition for Aqueous Solutions. Curve A is glycerine - water, curve B is propanol(n) - water. Note the change of scale magnitude as compared to Figure 25.

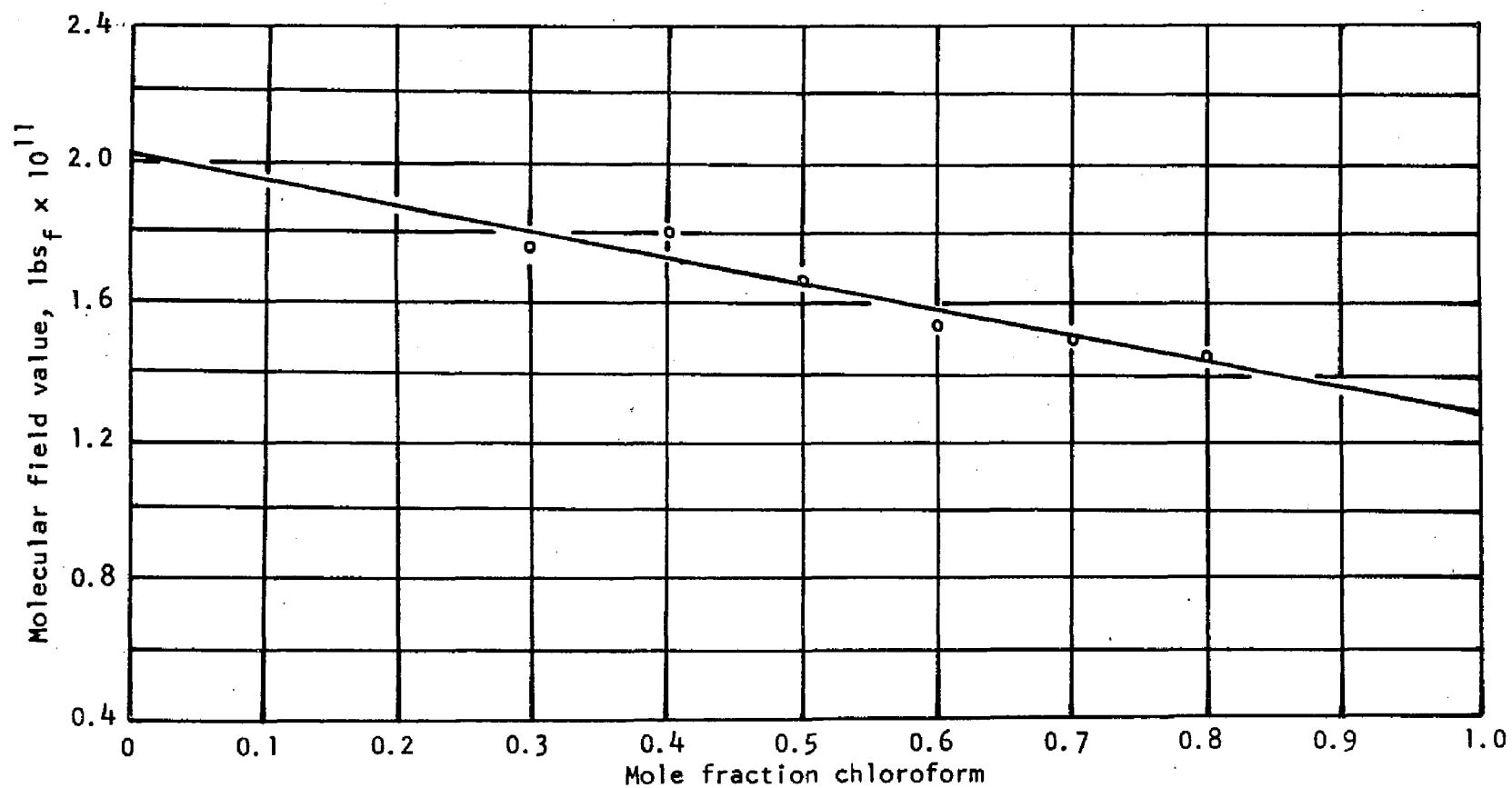


Figure 27. Molecular Field Value versus Composition for the Chloroform - Ethyl Ether System.

permit the accurate determination of F_m (see Chapter VI, Section 1).

The values determined are plotted in Figures 25 through 27.

The data plotted in the above listed Figures 16 through 27 appear in a tabulated arrangement in Appendix D.

The plots of the average molecular field values were extrapolated to the pure component compositions and eight pure component field values, F^* , were evaluated. Although six systems were extrapolated in this manner, there are only eight pure components since water was a common component in five of the systems. There were no other common components. The eight values of F^* are listed in Table I.

2) Prediction of the Thermal Conductivity of Binary Liquid Mixtures

According to the theory, the values of the molecular fields given in Table I permit the prediction of the thermal conductivity of a mixture of any two liquids which are miscible, by use of the method of Chapter II, Section 4. Consequently, two systems were made up of components listed in Table I, for which velocity of sound data were available and were studied in addition to the original eleven solutions. These systems are acetone-ethanol and acetone-chloroform. The predicted values of thermal conductivity, using the values of F^* previously determined, and the experimental values determined by the author, are presented in Tables II and III. The average of the absolute values of the errors for the two systems is 4.6%, with a maximum value of 7.0%.

TABLE I
MOLECULAR FIELD VALUES
at 25°C and 1 Atmosphere

Compound	F*, pounds force x 10 ¹¹
Acetone	3.3
Chloroform	1.30
Ethanol	2.22
Ethyl Ether	2.01
Glycerine	18.00
Methanol	1.49
Propanol(n)	4.50
Water	0.44

TABLE II
THERMAL CONDUCTIVITY VALUES
FOR THE ACETONE ETHANOL SYSTEM

at 25°C and 1 Atmosphere

Mole Fraction Acetone	$k_{\text{predicted}}$	k_{actual}	Error
0.0	0.0981	0.0981	---
0.1	0.0946	0.0974	-2.9%
0.2	0.0921	0.0969	-5.0%
0.3	0.0899	0.0963	-6.6%
0.4	0.0891	0.0958	-7.0%
0.5	0.0887	0.0953	-6.9%
0.6	0.0892	0.0949	-6.0%
0.7	0.0899	0.0944	-4.8%
0.8	0.0910	0.0940	-3.2%
0.9	0.0929	0.0936	-0.7%
1.0	0.0932	0.0932	---

Average of the absolute values of the error: 4.8%.

TABLE III
THERMAL CONDUCTIVITY VALUES
FOR THE ACETONE-CHLOROFORM SYSTEM
at 25°C and 1 Atmosphere

Mole Fraction Acetone	$k_{\text{predicted}}$	k_{actual}	Error
0.0	0.0687	0.0687	---
0.1	0.0662	0.0675	-1.9%
0.2	0.0644	0.0677	-4.9%
0.3	0.0645	0.0686	-6.0%
0.4	0.0658	0.0700	-6.0%
0.5	0.0680	0.0723	-6.0%
0.6	0.0705	0.0750	-6.0%
0.7	0.0753	0.0784	-4.0%
0.8	0.0800	0.0825	-3.0%
0.9	0.0858	0.0876	-2.0%
1.0	0.0930	0.0930	---

Average of the absolute values of the error: 4.4%.

In addition, the field values of Table I were used to re-calculate the thermal conductivity of each of the six systems as functions of composition. The predicted and experimental values, along with the error percentages, appear in Tables IV through IX.

The grand average of the absolute values of the errors in thermal conductivity prediction for all eight systems (72 points) is 3.6%, with a maximum value of 13%. The algebraic grand average of the errors is 0.05%, indicating no bias in the method.

3) Relationship of the Compressibility to the Field

Equation (34) relates the molecular field value of a pure liquid to its compressibility and size. The data are plotted as suggested by equation (34) in Figure 28, and are listed in Table XXIII, Appendix D. Available literature data on compressibility were used.¹¹ The point for chloroform was not considered in drawing the line as explained in Chapter VI, Section 1. The equation of the line is

$$F*Z = 263 r^2 - 0.96 \times 10^{-16} \quad (44)$$

4) Relationship of Viscosity to the Potential Function "m*"

In Chapter II, Section 7, a relationship between the potential function "m*" and viscosity for pure liquids is proposed. Values of "m*" were determined, as outlined in Chapter II, Section 7, and these values are plotted versus the viscosity and molecular size in Figure 29, as suggested by Equation (39). Tabulated data for Figure 29 appear in Table XXIV, Appendix D. The data yield a

TABLE IV
THERMAL CONDUCTIVITY VALUES
FOR THE METHANOL-WATER SYSTEM

at 25°C and 1 Atmosphere

Mole Fraction Methanol	$k_{\text{predicted}}$	k_{actual}	Error
0.0	0.350	0.350	---
0.1	0.299	0.295	+1.4%
0.2	0.262	0.250	+4.8%
0.3	0.230	0.218	+5.5%
0.4	0.203	0.192	+5.7%
0.5	0.178	0.171	+4.1%
0.6	0.158	0.153	+3.3%
0.7	0.144	0.141	+2.1%
0.8	0.132	0.131	+0.8%
0.9	0.123	0.122	+0.8%
1.0	0.116	0.116	---

Average of the absolute values of the error: 3.2%.

TABLE V
THERMAL CONDUCTIVITY VALUES
FOR THE ETHANOL-WATER SYSTEM
at 25°C and 1 Atmosphere

Mole Fraction Ethanol	$k_{\text{predicted}}$	k_{actual}	Error
0.0	0.350	0.350	---
0.1	0.267	0.264	+1.1%
0.2	0.204	0.211	-3.3%
0.3	0.168	0.180	-6.7%
0.4	0.150	0.155	-3.2%
0.5	0.136	0.137	-0.7%
0.6	0.125	0.123	+1.6%
0.7	0.115	0.114	+0.9%
0.8	0.107	0.107	0.0%
0.9	0.101	0.101	0.0%
1.0	0.097	0.097	---

Average of the absolute values of the error: 1.94%.

TABLE VI
THERMAL CONDUCTIVITY VALUES
FOR THE PROPANOL(n)-WATER SYSTEM
at 25°C and 1 Atmosphere

Mole Fraction Propanol	k _{predicted}	k _{actual}	Error
0.0	0.350	0.350	---
0.1	0.236	0.257	-8.0%
0.2	0.167	0.190	-12.0%
0.3	0.141	0.154	-8.0%
0.4	0.129	0.132	-2.0%
0.5	0.123	0.119	+5.0%
0.6	0.114	0.108	+6.0%
0.7	0.107	0.102	+5.0%
0.8	0.100	0.098	+2.0%
0.9	0.095	0.094	+1.0%
1.0	0.091	0.091	---

Average of the absolute values of the error: 5.4%.

TABLE VII
THERMAL CONDUCTIVITY VALUES
FOR THE GLYCERINE-WATER SYSTEM

at 25°C and 1 Atmosphere

CALCULATED ON THE BASIS OF A THREE BODY INTERACTION

Mole Fraction Glycerine	$k_{\text{predicted}}$	k_{actual}	Error
0.0	0.350	0.350	---
0.1	0.273	0.273	0.0%
0.2	0.233	0.233	0.0%
0.3	0.228	0.210	+8.4%
0.4	0.215	0.196	+9.6%
0.5	0.199	0.187	+6.5%
0.6	0.183	0.179	+2.4%
0.7	0.173	0.174	-0.6%
0.8	0.167	0.170	-1.8%
0.9	0.166	0.167	-0.6%
1.0	0.163	0.163	---

Average of the absolute values of the error: 3.3%.

TABLE VIII
THERMAL CONDUCTIVITY VALUES
FOR THE ACETONE-WATER SYSTEM

at 25°C and 1 Atmosphere

Mole Fraction Acetone	$k_{\text{predicted}}$	k_{actual}	Error
0.0	0.350	0.350	---
0.1	0.268	0.248	+8.0%
0.2	0.215	0.190	+13.0%
0.3	0.177	0.158	+12.0%
0.4	0.148	0.138	+7.0%
0.5	0.128	0.123	+4.0%
0.6	0.114	0.113	+1.0%
0.7	0.105	0.105	0.0%
0.8	0.100	0.100	0.0%
0.9	0.096	0.096	0.0%
1.0	0.093	0.093	---

Average of the absolute values of the error: 5%.

TABLE IX
THERMAL CONDUCTIVITY VALUES
FOR THE ETHYL ETHER-CHLOROFORM SYSTEM
at 25°C and 1 Atmosphere

Mole Fraction Chloroform	$k_{\text{predicted}}$	k_{actual}	Error
0.0	0.0799	0.0799	---
0.1	0.0783	0.0769	+1.8%
0.2	0.0753	0.0741	+1.6%
0.3	0.0717	0.0717	0.0%
0.4	0.0687	0.0696	-1.3%
0.5	0.0670	0.0676	-0.9%
0.6	0.0665	0.0665	0.0%
0.7	0.0668	0.0671	0.0%
0.8	0.0679	0.0679	0.0%
0.9	0.0703	0.0690	+1.9%
1.0	0.0705	0.0705	---

Average of the absolute values of the error: 0.8%

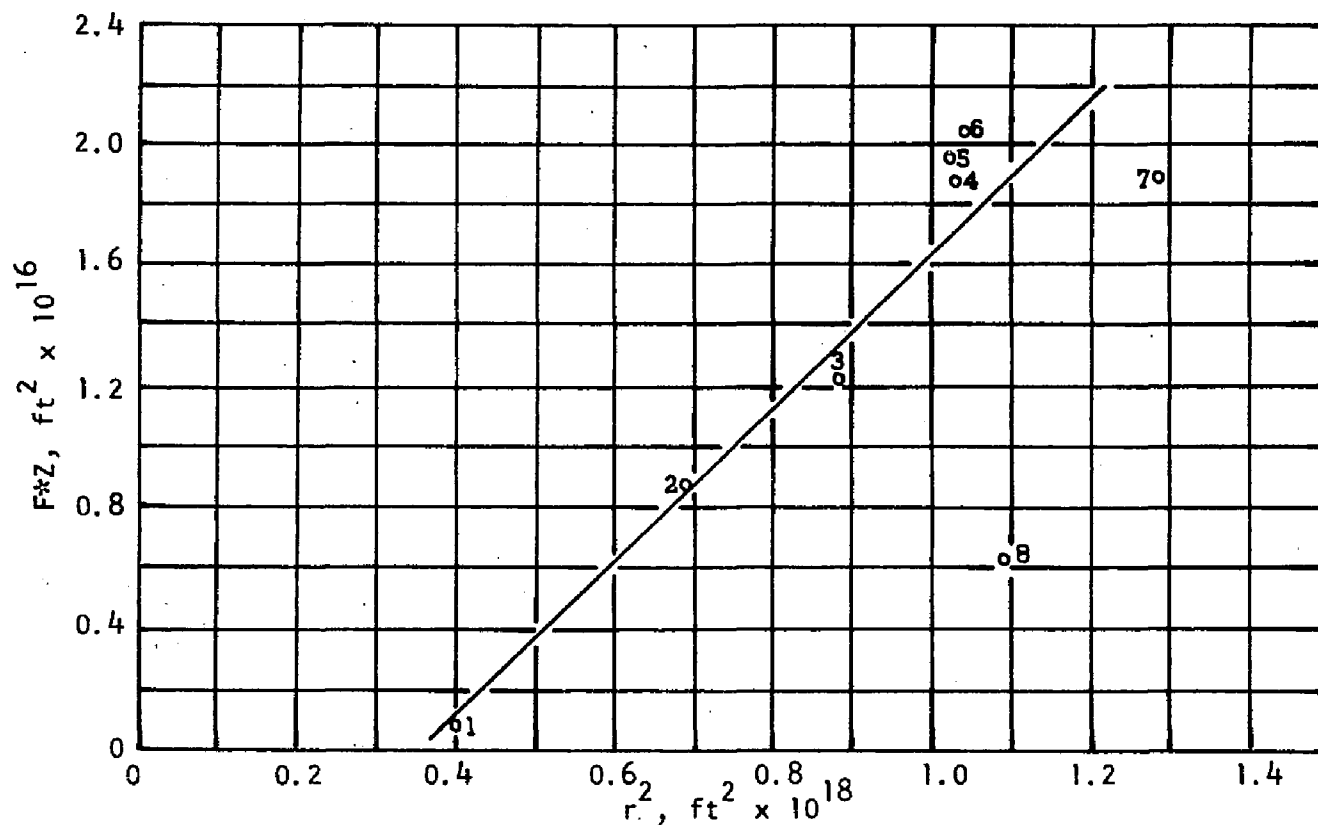


Figure 28. Generalized Correlation between Field, Compressibility, and Molecular Size. Points are: 1-water, 2-methanol, 3-ethanol, 4-glycerine, 5-acetone, 6-propanol(n), 7-ethyl ether, 8-chloroform. Point 8 was not considered in drawing the curve as explained in the text. Tabulated data are to be found in Table XXIII.

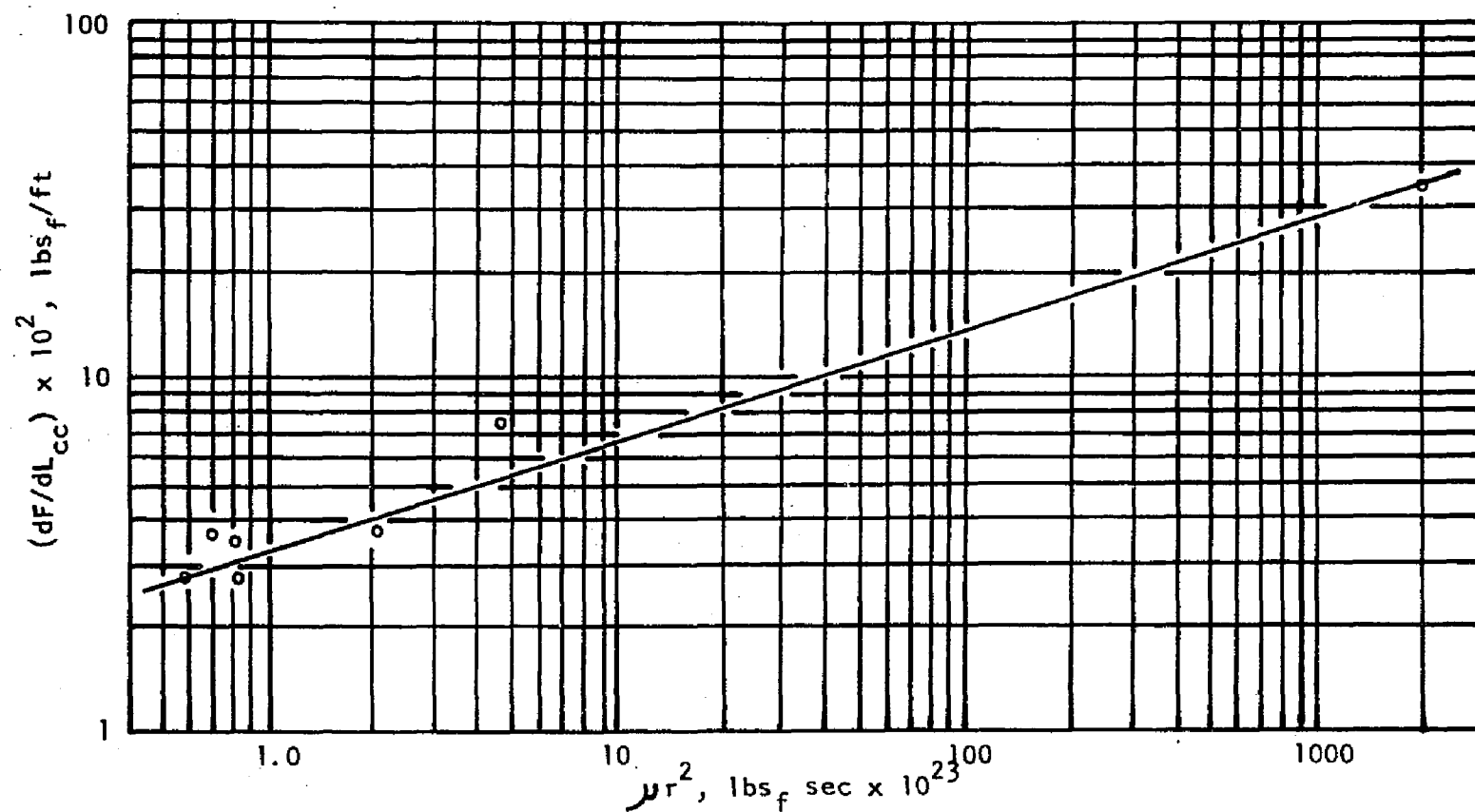


Figure 29. Generalized Correlation between dF/dL_{cc} , Viscosity, and Molecular Size. Compounds represented are methanol, ethanol, propanol(n), water, acetone, glycerine, and ethyl ether. Tabulated data are to be found in Table XXIV.

straight line on the log-log plot over a viscosity range of from 0.3 cp. to 1000 cp. The function found is:

$$m^* = 4.38 \times 10^5 (\mu r^2)^{0.3} \quad (45)$$

5) Relationship Between Viscosity and Compressibility

Equation (43) of Chapter II, Section 8, proposes that there is a relationship between viscosity, compressibility and molecular size. Such a relationship was found to exist within a family of compounds as shown by Figure 30, but no generalized relationship could be determined (see Chapter VI, Section 6). All data for Figure 30 were taken from the previously referenced literature. Tabulated data appear in Table XXV, Appendix D.

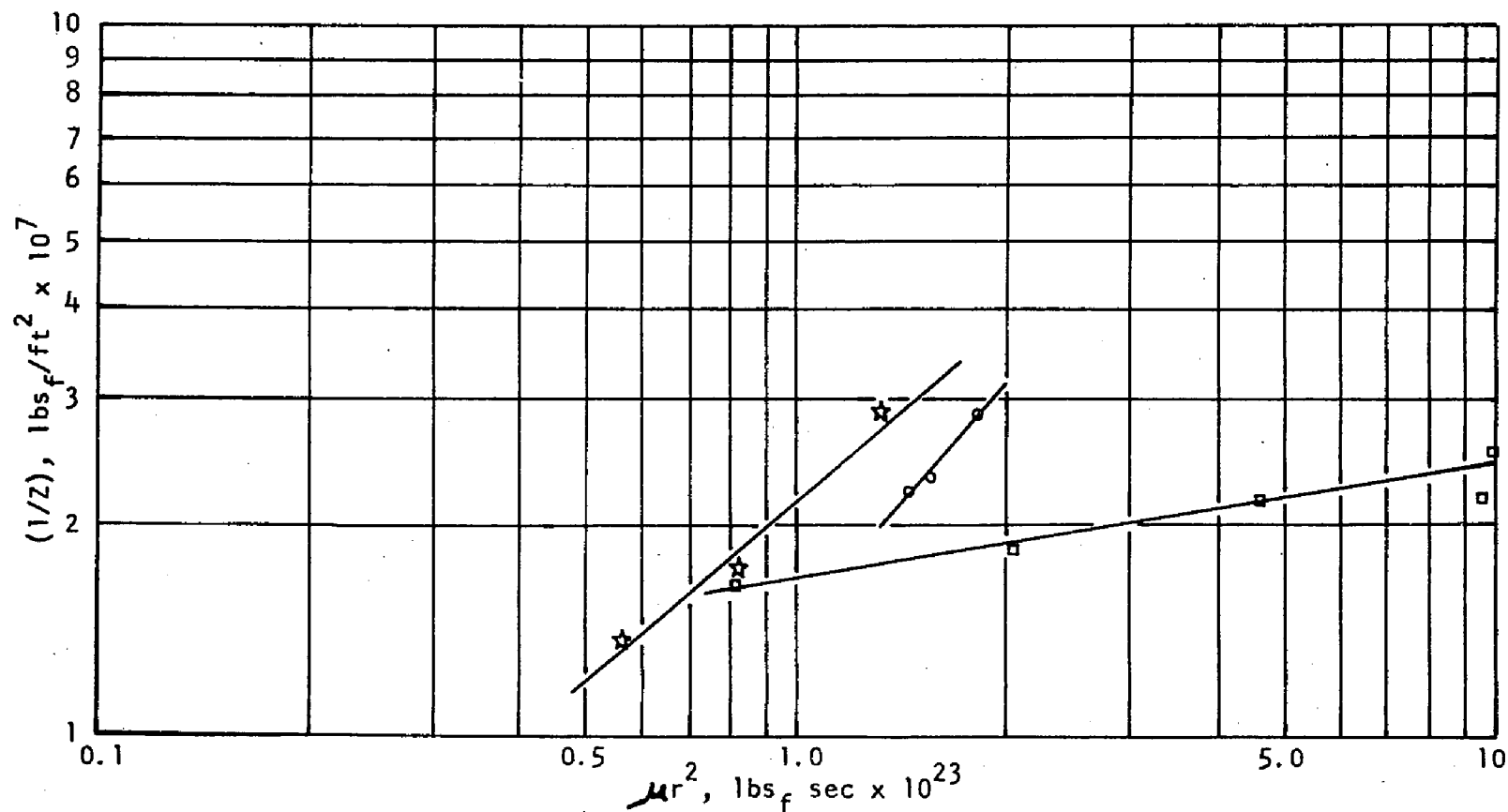


Figure 30. Correlation between Compressibility, Viscosity, and Molecular Size for Three Series of Compounds. Reading from left to right, the stars represent ethyl chloride, ethyl bromide, and ethyl iodide; the circles represent benzene, toluene, and xylene, and the squares represent methanol, ethanol, propanol(n), butanol(i), and amyl alcohol(i). Tabulated data are to be found in Table XXV.

CHAPTER VI

DISCUSSION

1) Calculation Error Propagation

Before the results can be discussed, it is necessary to consider the propagation of errors in the calculation of the excess intermolecular distance, for it is here that the greatest sensitivity to error arises.

The intermolecular distance is calculated from the four factors listed below, each with an estimated value of its typical percentage error:

k	-	$\pm 2\%$
C _p	-	$\pm 1\%$
U _s	-	$\pm 1\%$
ρ	-	essentially errorless

Since the intermolecular distance is obtained by processes of multiplication and division, the relative errors add, and the error expected in L is $\pm 4\%$.

The value of the ideal intermolecular distance is determined by the sum of the mole fractions (errorless) times the respective pure component intermolecular distances. In processes of addition and subtraction, the actual values of the errors add; hence to determine the error in L_i , it is necessary to choose a typical value for L.

Such a value is 0.250×10^{-9} ft. Then the actual value of the error in L is $\pm 0.010 \times 10^{-9}$ foot, and in L_i is $\pm 0.020 \times 10^{-9}$ foot.

L^E is determined by subtracting L from L_i . Since the actual error in L is (from above) $\pm 0.010 \times 10^{-9}$ foot and in L_i is $\pm 0.020 \times 10^{-9}$ foot, the uncertainty to be expected in L^E may be as high as $\pm 0.030 \times 10^{-9}$ foot.

Quite obviously, any system for which the calculations yield an excess intermolecular distance of less than 0.030×10^{-9} foot cannot be used for the determination of the molecular field values, because such a small deviation could be the result of experimental error alone.

On the basis of the foregoing, five of the original systems had to be rejected. Reference to Figures 20 and 21 will illustrate the point. The systems discarded were: acetic acid-water, ethyl-ether-benzene, ethylene glycol-water, carbon tetrachloride-benzene, and acetone-benzene. The ethylether-chloroform system (Figure 20) was included in the study, even though the error in its maximum value of the excess intermolecular distance could possibly be as high as 50%, and the error in its field values even greater by the contribution of the error in the excess free energy. For this reason, point 8 of Figure 28 was not considered in drawing the line, and point 7 was given little weight.

The maximum value of the excess intermolecular distance for all the aqueous solutions is typically 0.100×10^{-9} foot, which

gives an expected error of approximately $\pm 30\%$.

It must be borne in mind that the error percentage given above are maxima and that the actual error in the values is probably considerably less.

Error in the excess free energy values is difficult to estimate. Because of the impossibility of having vapor-liquid equilibrium data for a system at both one atmosphere and 25°C , the values of the excess free energy also cannot be at one atmosphere and 25°C . In the calculation of the activity coefficients, the values of temperature and pressure at which the data were taken were used. The activity coefficients so obtained were not corrected in any way. However, when these values were substituted into the equation for excess free energy (equation 23), the value of the temperature used was 25°C . Most of the vapor-liquid equilibrium data were available at one atmosphere; those systems for which it was not available at one atmosphere are so noted in Tables X through XXIII, Appendix D.

In view of the above, it would be expected that the maximum error in the molecular field values would be from $\pm 30\%$ to $\pm 40\%$. However, in the light of the correlations obtained, it is evident that the actual error is much less; a realistic, judicious estimate would be $\pm 20\%$.

If the error in the molecular field values of Table I be considered $\pm 20\%$, then the expected error in a predicted value of the thermal conductivity can be determined. If G^E were in error by

$\pm 5\%$, and F_m by $\pm 20\%$, then L^E would be in error by $\pm 25\%$. L_i must be assumed errorless in this case, since the predicted value is to be compared with "errorless" experimental values, from which L_i is determined. Consequently, the error in L^E would be $\pm 0.015 \times 10^{-9}$ ft., using 0.07×10^{-9} foot as a typical value of L^E , and the error in L would also be $\pm 0.015 \times 10^{-9}$ ft., or, typically, $\pm 6\%$. This would also be the expected error in the predicted thermal conductivity arising from the $\pm 20\%$ error in the field values and the method of estimation of F_m . Since the actual average error obtained for 72 predicted points was only 3.6%, the estimate of $\pm 20\%$ error in the field values is probably conservative.

One more statement may be made concerning error. If there were a large algebraic average error in the prediction, then it might be said that the method of prediction is biased either high or low. That the grand algebraic average error for the 72 predicted points is only 0.05% is indicative of an unbiased method of prediction.

2) General Usefulness of the Method for Predicting Thermal Conductivity of Solutions

The method presented here for predicting thermal conductivity is relatively inconvenient because of the large amount of data required, some of it difficult to obtain. These data are heat capacity, velocity of sound, density, molecular field values, vapor-liquid equilibrium data, and a knowledge of whether a two- or three-body interaction is involved. The numerous data required also introduce

error, and the method cannot be considered as reliable as the empirical method of Jordan and Coates.¹⁰

However, the method has its merits in the theoretical foundation and in the reasonable error of $\pm 6\%$ ($\pm 4\%$ in L , 1% in heat capacity, 1% in velocity of sound). It makes possible further advanced study of the liquid state through its evaluation of molecular fields and field slopes.

3) Mode of Interaction

The choice of two-body or three-body, or even four-body interaction, has not been completely resolved. All systems for which the thermal conductivity was predicted were calculated on the basis of a two-body interaction, with the exception of glycerine-water, which required a three-body interaction calculation. McAllister¹² encountered the same difficulty in his work on viscous interactions. McAllister arbitrarily chose a molecular diameter ratio of 1.5 as the dividing line. Above 1.5 was to be three-body or more, below 1.5 was to be two-body.

The glycerine-water system has a molecular radius ratio of 1.6, in agreement with McAllister's finding; acetone-water also has a molecular radius ratio of 1.6 but requires only a two-body interaction. McAllister found that for his viscosity correlation, acetone-water was best suited by a four-body interaction.

The conclusion reached by comparison with McAllister's work on viscosity is that the role played by molecular size and shape in

viscous interaction is quite different from that in the heat conduction interaction. This is further borne out by the findings discussed in Sections 4, 5, and 6 of this chapter.

The criterion for deciding the choice between two-body or three-body interaction has not been determined.

4) Relationship of the Compressibility to the Field Value

Figure 28 illustrates the generalizes correlation between field, compressibility and molecular size. The linear function yielded by the data points is in complete accord with the linear function predicted by the theory. Point 8 for chloroform was discredited as discussed in Section 1 of this chapter.

In the integration of the theoretical equation (30) the compressibility was assumed to be constant. It is not a constant, but varies with pressure, decreasing as pressure increases. However, all values of the compressibility used were determined at one atmosphere, as were the field values and molecular sizes; thus no error is introduced by this assumption.

There are two reasons for the lack of a perfect correlation. One is the error in the value of the fields. This alone is sufficient to account for the scatter in the plot, which is of the order of magnitude of 5%. The other source of error is that the molecular radius is not truly representative of the molecular size. Rectangular molecules, various orientations within the liquid, and packing effects all contribute additional scatter.

It was proposed in Chapter II that this correlation might be a possible way to predict molecular fields. This seems to be the case. Equation (44), determined from this plot, yields values of the field to within $\pm 5\%$, assuming errorless density and compressibility data. This, combined with the $\pm 20\%$ uncertainty in the experimental values, leads to a $\pm 8\%$ error in L , or a $\pm 8\%$ error in the estimated value of thermal conductivity arising from the method of prediction. This is entirely reasonable. The method deserves further development and refinement.

5) Relationship of Viscosity to the Potential Function "m"

A correlation between viscosity, molecular size, and the slope of the field, dF/dL_{CC} , termed "m", was found as illustrated in Figure 29, and as predicted in Chapter II. Scatter in the correlation is quite large, of the order of 15%.

Probably the major cause of the scatter in this correlation is the assumption of spherical molecules. The molecular shape and configuration would certainly play a more significant part in viscosity, where one molecule must be moved past the entanglements of another, than in the comparatively motionless situations of thermal conduction and mechanical compression.

A second cause of the scatter is the difficulty of obtaining an accurate slope graphically. In the case of chloroform, dL_{CC}/dX is so close to zero that dF/dL_{CC} is indeterminate; it does not appear in Figure 29. For several other compounds, dL_{CC}/dX and dF^*/dX

were changing rapidly, contributing to the error in their estimation.

When the range of the correlation is considered, it takes on added significance. The viscosity ranges from 0.3 cp (acetone) to 1000 cp (glycerine). The correlation does appear to be a valid one, and warrants further development.

6) Relationship between Viscosity, Compressibility, and Molecular Size

Section 8 of Chapter II predicted a relationship of the type:

$$\mu r^2 = f(r/Z) \quad (43)$$

This correlation was attempted using data for approximately twenty liquids. At first it appeared to be a total failure, but then it was noticed that such a correlation did exist within a family of compounds. Three series of compounds are presented in Figure 30, and yield a quite good correlation.

The failure of a generalized correlation is again attributed to the use of the molecular radius as being representative of molecular size. It would seem from this correlation that the use of the molecular radius is permissible within a series of compounds. Apparently, it is just as representative of the molecular size for one member of the series as for another, and the relative roles in viscosity and compressibility are comparable from member to member.

This correlation might be completely generalized by the use of particular molecular sizes, shapes, and orientations. The success

for the series of compounds justifies such an investigation.

The ordinate of Figure 30 is not r/Z as suggested by equation (43), but rather $1/Z$. The primary reason for this is that it yields a better correlation. Equation (43) cannot be taken as being rigid because the quantity actually being represented by r on the left side of the equation might in fact be quite different from the quantity represented by r on the right side. (This is the relative role of r concept.) A second reason for plotting $1/Z$ is that a correlation which includes the same variable on both axes is usually questioned as being a poor test of data.

7) Additional Comment

Some of the excess free energies reported are positive, some are negative. All the systems exhibited a contraction of the intermolecular distance on mixing, which implies a positive field for some molecules, a negative field for others. The explanation for this seeming contradiction is that it is not proper to suppose that a contraction is necessarily the result of work done by the attractive field, it may indeed be work done on the repulsive field. As explained in Appendix C, the field values reported are absolute values, because at the point of equilibrium, the attractive and repulsive fields must be equal and of opposite sign.

CHAPTER VII

CONCLUSION

As a result of this investigation, a valid method for predicting the thermal conductivity of a solution as a function of composition has been developed. As an outgrowth of the main effort, three additional correlations have been developed, relating the factors viscosity, compressibility, molecular size, molecular field and derivative of the field with respect to distance.

As a direct consequence of these findings, several areas for investigation and research have opened.

First, an investigation of the role of molecular size, shape, and orientation should be made. Perhaps by assigning definite configurations to the molecules, correlations such as equations (44) and (45) could be improved, and the relationships of Figure 31 generalized.

Second, more data should be gathered as it becomes available and used to further substantiate the theory. The present success of the correlations certainly warrants this.

Finally, and most important of all, an attempt should be made to relate all physical properties and characteristics of pure liquids and mixtures, such as density, diffusivity, interfacial tension, heat capacity, velocity of sound, vapor pressure, to four factors which characterize any liquid: molecular field, the derivative of the

molecular field with respect to distance, the molecular mass, and the molecular size (including shape, orientation, and intermolecular distances). Generalized correlations of this nature, such as were developed here for viscosity and compressibility, would be a great advance in the prediction of physical properties and would further the understanding of the liquid state.

SELECTED BIBLIOGRAPHY

1. Barratt, T., and Nettleton, H. R., International Critical Tables. New York: McGraw-Hill Book Co., 1929.
2. Chu, J. C., Wang, S. L., and Levy, S. L., Vapor Liquid Equilibrium Data. Ann Arbor, Michigan: J. W. Edwards, 1956.
3. Fillippov, L. V., and Novoselova, N. S., "The Thermal Conductivity of Solutions of Normal Mixtures," Vestnik Moskovskogo Universiteta. Seriya Fiziko-Matenateches Kikhi Estestvennvkk Nauk, No. 2, X(No. 3, 1955), pp. 37-40.
4. Fillippov, L. P., "Thermal Conductivity of Solutions of Associated Liquids," Vestnik Moskovskogo Universiteta. Seriya Fiziko-Matenateches Kikhi Estestvennvkk Nauk, (No. 5, 1955), pp. 67-69.
5. Frenkel, J., Kinetic Theory of Liquids. Oxford University Press, 1946.
6. Glasstone, S., The Elements of Physical Chemistry. New York: D. Van Nostrand Co., 1946.
7. Handbook of Chemistry and Physics, 29th Ed. Cleveland, Ohio: Chemical Rubber Publishing Co., 1945.
8. Hirschfelder, J. O., Curtiss, C. F., and Bird, R. B., Molecular Theory of Gases and Liquids. New York: John Wiley and Sons, Inc., 1954.
9. Hougen, O. A., and Watson, K. M., Chemical Process Principles, Part II. New York: John Wiley and Sons, Inc., 1947.
10. Jordan, H. B., "Prediction of Thermal Conductivity of Miscible Binary Liquid Mixtures from the Pure Component Values," Masters Thesis, Louisiana State University, 1961.

11. Landolt-Bornstein, Physikalisch Chemische Tabellen. Berlin: Julius Springer, 1927.
12. McAllister, R. A., "The Viscosity of Liquid Mixtures," A.I. Ch.E. Journal, VI (1960), pp. 427-431.
13. Perry, J. H., Chemical Engineers' Handbook, 3rd Edition. New York: McGraw-Hill Book Co., 1950.
14. Prigogine, I., The Molecular Theory of Solutions. New York: Interscience Publishers, Inc., 1957.
15. Riedel, L., Mitteilungen des Kaltetechnischen Instituts und der Reichforchungs--Anstalt fur Lebensmittelfrischaltung an der Technischen Hochschule Karlsruhe, No. 2, 1947, p. 45.
16. _____, "Warmeleitfähigkeitsmessungen an Mischungen Verschiedener Organischer Verbindungen mit Wasser," Chemie Ingenieur Technik, XXIII (1951), pp. 465-469.
17. Rodriguez, H. V., "Thermal Conductivity of Solutions as a Function of Temperature and Composition," Masters Thesis, Louisiana State University, 1958.
18. Sakiadis, B. C., and Coates, J., A Literature Survey of the Thermal Conductivity of Liquids. Engineering Experiment Station, Louisiana State University, Baton Rouge, La., 1952.
19. _____, A Literature Survey of the Thermal Conductivity of Liquids, Supplement of Part I. Engineering Experiment Station, Louisiana State University, Baton Rouge, La., 1953.
20. _____, Studies of Thermal Conductivity of Liquids, Part II, An Investigation of Factors Affecting the Design of a Liquid Thermoconductimetric Apparatus, Engineering Experiment Station, Louisiana State University, Baton Rouge, La., 1953.
21. _____, Studies of Thermal Conductivity of Liquids, Part III, A Thermoconductimetric Apparatus for Liquids, Engineering Experiment Station, Louisiana State University, Baton Rouge, La., 1954.
22. _____, Studies of Thermal Conductivity of Liquids, Part IV, A Literature Survey of Ultrasonic Velocities in Liquids and Solutions, Engineering Experiment Station, Louisiana State University, Baton Rouge, La., 1954.

23. _____, "Studies of Thermal Conductivity of Liquids,"
A.I.Ch.E. Journal, 1 (1955), p. 275.
24. Timmermans, J., The Physico-Chemical Constants of Binary Systems in Concentrated Solutions, New York: Interscience Publishers, Inc., 1959.

A P P E N D I X

APPENDIX A

NOMENCLATURE

A	-	area, ft^2
C _p	-	heat capacity, $\text{Btu/lb}_m\text{-}^\circ\text{F}$
c ₁	-	a constant of integration
c ₂	-	a constant of integration
D	-	deviation constant of the Jordan-Coates equation, dimensionless
d ₁ , d ₂	-	diameters of the hard molecules of solution components 1 and 2, respectively, feet
F	-	force, pounds force
F	-	field, a vector quantity, pounds force
F*	-	pure liquid molecular field, defined with respect to an average molecule, pounds force
F _m	-	average molecular field in a solution, defined with respect to an average molecule, pounds force
F _A *, F _B *	-	pure liquid molecular fields of solution components A and B, respectively, pounds force
F _{AB}	-	Geometric mean of F _A * and F _B *, pounds force
f	-	to be read "is a function of"; as a subscript, force
G	-	free energy, Btu/lb, mole
G _i	-	free energy of mixing for an ideal solution, Btu/lb, mole

G^E	-	excess free energy of mixing, $(G - G_i)$, Btu/lb. mole
H	-	enthalpy, Btu/lb. mole
k	-	thermal conductivity, Btu/hr-ft ² -°F/ft
k_1, k_2, k_s	-	thermal conductivities of components 1 and 2 of a solution, and of the solution, respectively, Btu/hr-ft ² -°F/ft
L	-	surface to surface intermolecular distance, feet
L_{cc}	-	center to center intermolecular distance, feet
L_1, L_2	-	surface to surface intermolecular distances for the solution components 1 and 2, respectively, feet
L_i	-	ideal surface to surface intermolecular distance, a linear function of mole fraction, feet
L^E	-	excess intermolecular distance, $(L_i - L)$, feet
m	-	slope of the molecular field with respect to distance, (dF^*/dL_{cc}) at the point where the net field is zero, lbs _f /ft; as a subscript, mass
M	-	molecular weight
N	-	Avagadro's Number, 2.73×10^{26} molecules per pound mole
P	-	pressure, pounds force/ft ²
P^*	-	vapor pressure, lb _f /ft ²
Q	-	heat content, Btu/lb. mole
q	-	rate of heat transfer, Btu/hr
R	-	ideal gas law constant, 1.987 Btu/lb. mole °R
r	-	molecular radius, calculated from density assuming spherical molecules, feet
S	-	in equations (16), (17), (18): entropy, Btu/lb. mole-°F; elsewhere: distance, feet

T	-	temperature, $^{\circ}\text{R}$
T_1, T_2	-	temperature at points 1 and 2, respectively, $^{\circ}\text{R}$
U	-	energy drop per molecule, Btu/molecule
U_s	-	velocity of sound, feet/sec
u	-	velocity, feet/sec
V	-	volume, ft^3
W_m	-	maximum work per mole, Btu/lb. mole
W_{mi}	-	maximum work of mixing an ideal solution, Btu/lb. mole
w_1, w_2	-	weight fractions of solution components 1 and 2, respectively
X	-	mole fraction
x_1, x_2	-	mole fractions of solution components 1 and 2, respectively
y	-	distance used in defining the velocity gradient for viscosity, feet
Z	-	compressibility, ft^2/lb_f

Greek Symbols:

γ_1, γ_2	-	activity coefficients of solution components 1 and 2, respectively
Δ	-	difference or change in
μ	-	viscosity, $\text{lbs}_f\text{-sec}/\text{ft}^2$
ρ	-	density, lbs_m/ft^3
τ	-	shear stress, lbs_f/ft^2
π	-	constant, 3.14

APPENDIX B

SAMPLE CALCULATIONS

The ethanol-water system at 0.6 mole fraction ethanol will be used to illustrate the calculations.

1. Intermolecular distance

$$L = \frac{k}{C_p \rho U_s}$$

$$L = \frac{0.123}{(0.73)(52.5)(15.55 \times 10^6)}$$

$$L = 0.206 \times 10^{-9} \text{ ft.}$$

2. Ideal intermolecular distance

$$L_{H_2O} = \left(\frac{k}{C_p \rho U_s} \right)_{H_2O}$$

$$L_{H_2O} = \frac{0.350}{(1)(62.24)(17.68 \times 10^6)}$$

$$L_{H_2O} = 0.318 \times 10^{-9} \text{ ft.}$$

$$L_{EtOH} = \left(\frac{k}{C_p \rho U_s} \right)_{EtOH}$$

$$L_{EtOH} = \frac{0.097}{(0.575)(49.00)(14.5 \times 10^6)}$$

$$L_{EtOH} = 0.237 \times 10^{-9} \text{ ft.}$$

$$L_i = X_{H_2O} L_{H_2O} + X_{EtOH} L_{EtOH}$$

$$L_i = (0.4)(0.318) + (0.6)(0.237) \times 10^{-9}$$

$$L_i = 0.267 \times 10^{-9} \text{ ft.}$$

3. Excess intermolecular distance

$$L^E = L_i - L$$

$$L^E = (0.267 - 0.206) \times 10^{-9}$$

$$L^E = 0.061 \times 10^{-9} \text{ ft.}$$

4. Excess free energy

The calculation of excess free energy was performed on an IBM 650 computer, according to the following method. Available data points were used; the final values of G^E were taken from curves constructed through the points. The data used in the calculations below are taken from such curves.

$$\gamma_{H_2O} = \frac{y_P}{x P^*}$$

$$\gamma_{H_2O} = \frac{(0.300)(2117)}{(0.4)(989)}$$

$$\gamma_{H_2O} = 1.60$$

P^* was evaluated at 80°C , the temperature of the system at which the compositions were evaluated.

A similar calculation was made for ethanol, yielding:

$$\gamma_{EtOH} = 1.131$$

$$G^E = RT (x_1 \ln \gamma_1 + x_2 \ln \gamma_2)$$

$$G^E = (1.987)(536)(0.6 \ln 1.131 + 0.4 \ln 1.60)$$

$$G^E = 279 \text{ Btu/lb. mole}$$

5. Average molecular field

$$F_m = \frac{G^E}{N L^E}$$

$$F_m = \frac{(279)(778)}{(0.061 \times 10^{-9})(2.73 \times 10^{26})}$$

$$F_m = 1.30 \text{ lbs}_f/\text{molecule}$$

6. Prediction of thermal conductivity

Plots of F_m versus composition were extrapolated to yield the values of F^* in Table I. For this system

$$F^*_{\text{EtOH}} = 2.22 \times 10^{-11} \text{ lbs}_f$$

$$F^*_{\text{H}_2\text{O}} = 0.44 \times 10^{-11} \text{ lbs}_f$$

Estimation of F_m at 0.6 mole fraction ethanol, using two body interaction:

$$F_m = x_1^2 F_1^* + 2x_1 x_2 \sqrt{F_1^* F_2^*} + x_2^2 F_2^*$$

$$F_m = (0.36)(2.22) + 0.48 \sqrt{(2.22)(0.44)} + 0.16(0.44) \\ \times 10^{-11}$$

$$F_m = 1.34 \times 10^{-11} \text{ lbs}_f$$

$$L^E = \frac{G^E}{F_m N}$$

$$L^E = \frac{(279)(778)}{(1.34 \times 10^{-11})(2.73 \times 10^{26})}$$

$$L^E = 0.059 \times 10^{-11} \text{ ft}$$

$$L = L_i - L^E$$

$$L = (0.267 - 0.059) \times 10^{-11}$$

$$L = 0.208 \times 10^{-11} \text{ ft}$$

$$k = C_p \rho U_s L$$

$$k = (0.73)(52.5)(15.55 \times 10^6)(0.208 \times 10^{-11})$$

$$k = 0.125 \text{ Btu/hr-ft}^2\text{-}^\circ\text{F/ft}$$

$$\text{Error} = \frac{(k_{\text{predicted}} - k_{\text{actual}})}{k_{\text{actual}}} \times 100$$

$$\text{Error} = \frac{0.125 - 0.123}{0.123}$$

$$\text{Error} = 1.6\%$$

7. Molecular radius

For water, $\rho = 62.42 \text{ lbs}_m/\text{ft}^3$

$$\text{Volume per molecule} = \frac{M}{\rho N}$$

$$\text{Volume per molecule} = \frac{18}{(62.42)(2.73 \times 10^{26})}$$

$$\text{Volume per molecule} = 1.06 \times 10^{-27} \text{ ft}^3$$

$$r_{\text{H}_2\text{O}} = \frac{(0.75)(\text{volume per molecule})}{M}^{1/3}$$

$$r_{\text{H}_2\text{O}} = \frac{(0.75)(1.06 \times 10^{-27})}{3.14}^{1/3}$$

$$r_{\text{H}_2\text{O}} = 0.633 \times 10^{-9} \text{ ft}$$

APPENDIX C
NOTES ON FIELD THEORY

A force field may be defined mathematically as:

$$F = \frac{dW_m}{dS} \quad (46)$$

This equation states that the numerical value of the field represents the amount of work necessary to move a differential distance within the field, provided that the motion is in part, parallel to the field. This value must be defined with respect to something, for the question immediately arises, move what in the field? Consider the gravitational field of the earth. It is not uniform with distance, so in order to define it, some reference point in the field must be chosen. This point is usually taken as sea level. The gravitational field at sea level is numerically one pound force, defined with respect to one pound mass, or the field is one pound force per pound mass.

If the motion is always parallel to the field (vertical motion), then equation (46) may be integrated, assuming a constant field, to give:

$$\Delta W_m = F \Delta S$$

W_m is termed the potential energy difference, or simply the

potential difference, expressed on the basis of one pound mass. If five pounds mass were to be moved two feet, parallel to the earth's gravitational field of one pound force per pound mass, then the work done would be:

$$\text{Total work} = \frac{1 \text{ pound force}}{\text{pound mass}} (2 \text{ feet})(5 \text{ pounds mass})$$

$$\text{Total work} = 10 \text{ foot pounds force}$$

Suppose a weight rests on a table. The net force on the weight is zero. The field of gravity is acting upon the weight, but there is an opposing "field" exerted by the table which is exactly equal to, but of opposite sign from the gravitational field, provided both fields are defined with respect to the same reference. The net field is zero, but it cannot be said that the two opposing fields do not exist.

The two fields above both vary with distance, but in very different manners. The earth's field is considered uniform over reasonable distances, whereas the table's repulsive field rises from zero very sharply. However, at the point of rest of the weight, the two fields are equal, and an infinitesimal motion in either vertical direction would require the same amount of work.

The net field may be zero, but the absolute values of the fields are identical. It is this absolute value of either field which is referred to in this work.

These absolute values of the molecular fields presented in Table I are defined with respect to a similar molecule. For a

solution, the average field value is the field of the average molecule, defined in Chapter II, Section-2, with respect to another similar average molecule.

Just as it was necessary to specify sea level as the point of measurement of the earth's gravitational field, a point of measurement must be chosen for the molecular fields. All that can be said concerning this is that the value of the fields found are those at which the molecules experience no net force, when at 25°C and one atmosphere pressure.

APPENDIX D

TABULATED RESULTS

TABLE X

RESULTS FOR THE METHANOL-WATER SYSTEM

at 25°C and 1 Atmosphere

Mole Fraction Methanol	L ft x 10 ⁹	L ^E ft x 10 ⁹	G ^E Btu/lb mole	F _m lbs force x 10 ¹¹
0.0	0.318	0.000	0	(0.44)
0.1	0.267	0.049	82	0.48
0.2	0.241	0.073	130	0.51
0.3	0.232	0.079	159	0.57
0.4	0.233	0.075	175	0.67
0.5	0.239	0.067	180	0.76
0.6	0.248	0.057	170	0.85
0.7	0.260	0.043	149	0.98
0.8	0.273	0.027	103	1.09
0.9	0.284	0.013	59	1.30
1.0	0.296	0.000	0	(1.49)

Values in parentheses were obtained by extrapolation.

TABLE XI
RESULTS FOR THE ETHANOL-WATER SYSTEM
at 25°C and 1 Atmosphere

Mole Fraction Ethanol	L ft x 10 ⁹	L ^E ft x 10 ⁹	G ^E Btu/lb mole	F _m lbs force x 10 ¹¹
0.0	0.318	0.000	0	(0.44)
0.1	0.225	0.085	162	0.54
0.2	0.204	0.098	254	0.74
0.3	0.203	0.095	302	0.91
0.4	0.200	0.087	322	1.05
0.5	0.202	0.075	313	1.19
0.6	0.206	0.061	279	1.30
0.7	0.216	0.045	234	1.48
0.8	0.225	0.029	175	1.72
0.9	0.231	0.014	99	2.01
1.0	0.237	0.000	0	(2.22)

Values in parentheses were obtained by extrapolation.

TABLE XII
RESULTS FOR THE PROPANOL(n)-WATER SYSTEM
at 25°C and 1 Atmosphere

Mole Fraction Propanol	L ft x 10 ⁹	L ^E ft x 10 ⁹	G ^E Btu/lb mole	F _m lbs force x 10 ¹¹
0.0	0.318	0.000	0	(0.44)
0.1	0.227	0.081	230	0.81
0.2	0.210	0.089	368	1.18
0.3	0.204	0.085	435	1.46
0.4	0.200	0.079	462	1.67
0.5	0.198	0.072	447	1.77
0.6	0.201	0.059	404	1.95
0.7	0.206	0.044	338	2.19
0.8	0.212	0.028	262	2.66
0.9	0.217	0.014	170	3.44
1.0	0.221	0.000	0	(4.50)

Values in parentheses were obtained by extrapolation.

TABLE XIII
RESULTS FOR THE ACETONE-WATER SYSTEM
at 25°C and 1 Atmosphere

Mole Fraction Acetone	L ft x 10 ⁹	L ^E ft x 10 ⁹	G ^E Btu/lb mole	F _m lbs force x 10 ¹¹
0.0	0.318	0.000	0	(0.44)
0.1	0.229	0.082	214	0.74
0.2	0.202	0.102	351	0.98
0.3	0.196	0.101	442	1.24
0.4	0.195	0.095	483	1.45
0.5	0.198	0.085	499	1.67
0.6	0.205	0.070	475	1.93
0.7	0.216	0.052	414	2.27
0.8	0.228	0.033	304	2.62
0.9	0.238	0.016	166	2.96
1.0	0.247	0.000	0	(3.30)

Values in parentheses were obtained by extrapolation.

TABLE XIV
RESULTS FOR THE GLYCERINE-WATER SYSTEM
at 25°C and 1 Atmosphere*

Mole Fraction Glycerine	L ft x 10 ⁹	L ^E ft x 10 ⁹	G ^E Btu/lb mole	F _m lbs force x 10 ¹¹
0.0	0.318	0.000	0	(0.44)
0.1	0.252	0.052	201	1.10
0.2	0.212	0.076	459	1.72
0.3	0.189	0.083	569	1.95
0.4	0.177	0.079	716	2.58
0.5	0.170	0.071	927	3.72
0.6	0.165	0.059	1138	5.49
0.7	0.163	0.045	1278	8.09
0.8	0.162	0.030	1229	11.66
0.9	0.161	0.015	787	14.94
1.0	0.161	0.000	0	(18.00)

Values in parentheses were obtained by extrapolation.

* G^E is at 50 mm Hg

TABLE XV
RESULTS FOR THE ETHYL ETHER-CHLOROFORM SYSTEM
at 25°C and 1 Atmosphere*

Mole Fraction Chloroform	L ft x 10 ⁹	L ^E ft x 10 ⁹	G ^E Btu/lb mole	F _m lbs force x 10 ¹¹
0.0	0.290	0.000	0	(2.01)
0.1	0.272	0.018	- 87	1.38
0.2	0.257	0.033	-189	1.63
0.3	0.246	0.044	-272	1.76
0.4	0.238	0.052	-328	1.80
0.5	0.232	0.058	-344	1.69
0.6	0.231	0.059	-319	1.54
0.7	0.240	0.050	-266	1.51
0.8	0.252	0.038	-192	1.44
0.9	0.268	0.022	- 81.2	1.05
1.0	0.289	0.000	0	(1.30)

Values in parentheses were obtained by extrapolation.

* G^E has a pressure range of from 143 to 397 mm Hg.

TABLE XVI
RESULTS FOR THE ACETONE-BENZENE SYSTEM
at 25°C and 1 Atmosphere

Mole Fraction Acetone	L ft x 10 ⁹	L ^E ft x 10 ⁹	G ^E Btu/lb mole	F _m lbs force x 10 ¹¹
0.0	0.233	*	0	**
0.1	0.238		20	
0.2	0.243		35	
0.3	0.248		48	
0.4	0.252		60	
0.5	0.255		65	
0.6	0.258		63	
0.7	0.259		50	
0.8	0.262		38	
0.9	0.264		25	
1.0	0.266		0	

* Essentially zero

** Indeterminant

TABLE XVII
RESULTS FOR THE ACETIC ACID-WATER SYSTEM
at 25°C and 1 Atmosphere*

Mole Fraction Acetic Acid	L ft x 10 ⁹	L ^E ft x 10 ⁹	G ^E Btu/lb-mole	F _m lbs force x 10 ¹¹
0.0	0.319	0.000	0	**
0.1	0.293	0.015	11	
0.2	0.272	0.026	29	
0.3	0.254	0.033	50	
0.4	0.238	0.038	74	
0.5	0.229	0.037	94	
0.6	0.222	0.033	106	
0.7	0.218	0.027	110	
0.8	0.215	0.019	94	
0.9	0.213	0.010	58	
1.0	0.212	0.000	0	

* G^E is at 20 mm Hg.

** L^E and G^E are too small to permit an accurate evaluation.

TABLE XVIII
RESULTS FOR THE BENZENE-CARBON TETRACHLORIDE SYSTEM
at 25°C and 1 Atmosphere*

Mole Fraction Benzene	L ft x 10 ⁹	L ^E ft x 10 ⁹	G ^E Btu/lb mole	F _m lbs force x 10 ¹¹
0.0	0.255	0.000	0	**
0.1	0.249	0.004	- 23	
0.2	0.244	0.009	- 45	
0.3	0.241	0.010	- 67	
0.4	0.238	0.013	- 83	
0.5	0.236	0.015	-108	
0.6	0.234	0.016	-131	
0.7	0.232	0.016	-144	
0.8	0.232	0.015	-142	
0.9	0.235	0.012	-113	
1.0	0.246	0.000	0	

* G^E is at a pressure of 1.00 mm Hg.

** L^E and G^E are too small to permit an accurate evaluation.

TABLE XIX
RESULTS FOR THE ETHYLENE GLYCOL-WATER SYSTEM
at 25°C and 1 Atmosphere*

Mole Fraction Glycol	L ft x 10 ⁹	L ^E ft x 10 ⁹	G ^E Btu/lb mole	F _m lbs force x 10 ¹¹
0.0	0.317	0.000	0	**
0.1	0.282	0.018	- 26	
0.2	0.265	0.023	- 52	
0.3	0.254	0.022	- 76	
0.4	0.246	0.018	-101	
0.5	0.237	0.015	-123	
0.6	0.227	0.013	-141	
0.7	0.217	0.011	-128	
0.8	0.206	0.010	- 95	
0.9	0.194	0.006	- 48	
1.0	0.192	0.000	0	

* G^E is at a pressure of 228 mm Hg.

** L^E and G^E are too small to permit an accurate evaluation.

TABLE XX
RESULTS FOR THE ETHYL ETHER-BENZENE SYSTEM
at 25°C and 1 Atmosphere*

Mole Fraction Ether	L ft x 10 ⁹	L ^E ft x 10 ⁹	G ^E Btu/lb mole	F _m lbs force x 10 ¹¹
0.0	0.249	0.000	0	**
0.1	0.228	0.022	200	
0.2	0.227	0.028	306	
0.3	0.228	0.031	372	
0.4	0.231	0.032	401	
0.5	0.238	0.030	418	
0.6	0.245	0.026	407	
0.7	0.256	0.019	376	
0.8	0.267	0.014	308	
0.9	0.277	0.007	183	
1.0	0.288	0.000	0	

* G^E has a pressure range from 150 to 760 mm Hg.

** L^E is too small to permit an accurate evaluation.

TABLE XXI
RESULTS FOR THE ACETONE-CHLOROFORM SYSTEM
at 25°C and 1 Atmosphere*

Mole Fraction Acetone	L ft x 10 ⁹	L ^E ft x 10 ⁹	G ^E Btu/lb mole	F _m lbs force x 10 ¹¹
0.0	0.274	0.000	0	**
0.1	0.259	0.013	92	
0.2	0.252	0.018	169	
0.3	0.249	0.020	221	
0.4	0.248	0.020	247	
0.5	0.251	0.015	247	
0.6	0.252	0.012	219	
0.7	0.253	0.010	178	
0.8	0.256	0.005	125	
0.9	0.259	0.001	68	
1.0	0.258	0.000	0	

* G^E has a pressure range of from 280 to 332 mm Hg.

** L^E is too small to permit an accurate evaluation.

TABLE XXII
RESULTS FOR THE ACETONE-ETHANOL SYSTEM
at 25°C and 1 Atmosphere

Mole Fraction Acetone	L ft x 10 ⁹	L ^E ft x 10 ⁹	G ^E Btu/lb mole	F _m lbs force x 10 ¹¹
0.0	0.241	0.000	0	*
0.1	0.241	0.001	67	
0.2	0.242	0.002	125	
0.3	0.243	0.003	168	
0.4	0.245	0.003	190	
0.5	0.246	0.003	197	
0.6	0.248	0.003	185	
0.7	0.250	0.003	157	
0.8	0.253	0.002	113	
0.9	0.253	0.004	61	
1.0	0.258	0.000	0	

* L^E is too small to permit an accurate evaluation.

TABLE XXIII
DATA FOR FIGURE 28

Compound	$\frac{F \cdot Z}{ft^2} \times 10^{16}$	$\frac{r^2}{ft^2} \times 10^{18}$
Water	0.088	0.401
Methanol	0.894	0.686
Ethanol	1.221	0.884
Propanol(n)	2.070	1.036
Chloroform	0.611	1.088
Acetone	1.947	1.024
Ethyl Ether	1.889	1.286
Glycerine	1.889	1.024

TABLE XXIV
DATA FOR FIGURE 29

Compound	$\frac{dF}{dL_{cc}} \times 10^2$ pounds force/ft	$r^2 \times 10^{-23}$ pounds force sec.
Methanol	2.67	0.82
Ethanol	3.71	2.03
Propanol(n)	7.50	4.65
Acetone	3.68	0.69
Water*	3.50	0.80
Glycerine	34.83	2022.00
Ethyl Ether	2.78	0.59

* Average of four values. Values of dF/dL_{cc} for water when mixed with glycerine, and for chloroform when mixed with ethyl ether, were indeterminant because dL_{cc}/dX approached zero.

TABLE XXV
DATA FOR FIGURE 30

Compound	$\frac{1}{Z}$ (lbs_f/ft^2) $\times 10^7$	r^2 ($\text{lbs}_f \text{ sec}$) $\times 10^{23}$
Ethyl Chloride	1.39	0.558
Ethyl Bromide	1.75	0.826
Ethyl Iodide	2.86	1.310
Benzene	2.22	1.455
Toluene	2.32	1.571
Xylene	2.86	1.818
Methanol	1.67	0.821
Ethanol	1.82	2.024
Propanol(n)	2.17	4.670
Butanol(i)	2.17	9.449
Amyl Alcohol(i)	2.50	10.64

APPENDIX E

INDEX TO LITERATURE DATA

	k	C _p		U _s	vap-liq eq
Acetone-Ethanol	a	24	1	22	2
Acetone-Chloroform	a	24	1	22	2
Methanol-Water	16	13	13	22	2
Ethanol-Water	16	13	13	22	2
Propanol(n)-Water	16	1	13	22	12
Glycerine-Water	16	13	1	22	2
Acetone-Water	16	1	13	22	2
Ethyl Ether-Chloroform	3	1	1	22	1
Acetone-Benzene	15	1	1	22	2
Acetic Acid-Water	18	1	1	22	2
Benzene-Carbon Tetrachloride	15	1	1	22	2
Ethylene Glycol-Water	16	1	7	22	12
Ethyl Ether-Benzene	3	1	1	22	23

Numbers refer to Bibliography entries. "a" refers to the author's determinations. All compressibilities for pure liquids were taken from 11; all viscosities for pure liquids were taken from 13.

VITA

The author was born August 30, 1932, in New Orleans, Louisiana. He attended elementary and high school there, and entered Louisiana State University in September, 1950. He received a Bachelor of Science Degree in the field of Chemical Engineering in August, 1954.

After receiving the B.S. degree, he was employed by the Natural Gas Department of the Magnolia Petroleum Company until January of 1955. At that time he was called to active duty with the United States Army as a 2nd Lieutenant in the Chemical Corps. He served two years as an instructor of physics and radiological defense at the Chemical Corps School, Fort McClellan, Alabama. It was there that he met the former Miss Jewel Taylor of Andalusia, Alabama. They were married in May of 1956.

The following January, the author was released from active duty, and returned to Louisiana State University as a graduate student. In August of 1958, he received a Master of Science degree in the field of Chemical Engineering. He is currently a candidate for the degree of Doctor of Philosophy in Chemical Engineering.

During the summers of 1957, 1958, and 1960, he was employed by Kaiser Aluminum, Ormet (Olin-Revere Metals), and Dow Chemical Company in various research and development positions.

He is a member of Phi Lambda Upsilon.

Upon completion of the academic work, the author plans to join the staff of the Field Research Laboratory of the Socony-Mobil Oil Company, Dallas, Texas.

EXAMINATION AND THESIS REPORT

Candidate: Harold Vernon Rodriguez

Major Field: Chemical Engineering

Title of Thesis: Molecular Field Relationships to Liquid Viscosity,
Compressibility, and Prediction of Thermal Conductivity
of Binary Liquid Mixtures.

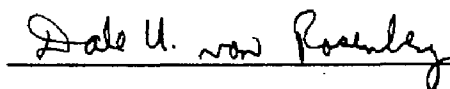
Approved:


Major Professor and Chairman

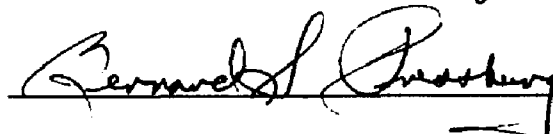

Dean of the Graduate School

EXAMINING COMMITTEE:









Date of Examination:
January 9, 1962